REPORT DOCUMENTATION PAGE

1a Report Security Classification Unclassified		1b Restrictive Markings			
2a Security Classification Authority		3 Distribution Availability of Report			
2b Declassification Downgrading Schedule		Approved for public release; distribution is unlimited.			
4 Performing Organization Report Number(s)		5 Monitoring Organization Report Number(s)			
6a Name of Performing Organization Naval Postgraduate School	6b Office Symbol (if applicable) 67	7a Name of Monitoring Organization Naval Postgraduate School			
6c Address (city, state, and ZIP code) Monterey, CA 93943-5000		7b Address (city, state, and ZIP code) Monterey, CA 93943-5000			
8a Name of Funding Sponsoring Organization	8b Office Symbol (if applicable)	9 Procurement Instrument Identification Number			
8c Address (city, state, and ZIP code)		10 Source of Funding Numbers			
		Program Element No	Project No	Task No	Work Unit Accession No

11 Title (include security classification) INITIAL FLIGHT TEST OF HALF-SCALE UNMANNED AIR VEHICLE

12 Personal Author(s) Kee, Yeho

13a Type of Report Master's Thesis	13b Time Covered From To	14 Date of Report (year, month, day) September 1989	15 Page Count 67

16 Supplementary Notation The views expressed in this thesis are those of the author and do not reflect the official policy or position of the Department of Defense or the U.S. Government.

17 Cosati Codes			18 Subject Terms (continue on reverse if necessary and identify by block number)
Field	Group	Subgroup	Flight test, UAV, RPV, Performance, Drag-Polar, Thrust Coefficient, Power Curve

19 Abstract (continue on reverse if necessary and identify by block number)

Pioneer, a short-range Unmanned Air Vehicle, was recently introduced into fleet operations. Due to the manner of test and evaluation of UAV's, problems with the air vehicle have been identified during, rather than prior to, operational use and contractor testing. A flight research program has begun at the Naval Postgraduate School to use a half-scale Pioneer UAV in an attempt to study the flight behavior of Pioneer. Limitation of flight endurance below original estimations has prompted a drag analysis of the vehicle to be performed. Previously, wind tunnel work was carried out for propeller studies. The current investigation uses the results of that work to complete flights for determination of a drag polar for the vehicle. A drag clean-up of the original wing configuration was performed, and though the data are scattered due to the measurement techniques, trends indicate a significant reduction in drag for the new wing. Comparison of the drag data with numerical predictions shows a reasonable correlation.

20 Distribution Availability of Abstract ☒ unclassified unlimited ☐ same as report ☐ DTIC users	21 Abstract Security Classification Unclassified	
22a Name of Responsible Individual Richard M. Howard	22b Telephone (include Area code) (408) 646-2870	22c Office Symbol Code 67 Ho

i

T245269

Initial Flight Test of half-scale Unmanned Air Vehicle

by

Kee, Yeho
Major, Korean Air Force
B.S., Korean Air Force Academy, 1978

Submitted in partial fulfillment of the
requirements for the degree of

MASTER OF SCIENCE IN AERONAUTICAL ENGINEERING

from the

NAVAL POSTGRADUATE SCHOOL
September 1989

ABSTRACT

Pioneer, a short-range Unmanned Air Vehicle, was recently introduced into fleet operations. Due to the manner of test and evaluation of UAV's, problems with the air vehicle have been identified during, rather than prior to, operational use and contractor testing. A flight research program has begun at the Naval Postgraduate School to use a half-scale Pioneer UAV in an attempt to study the flight behavior of Pioneer. Limitation of flight endurance below original estimations has prompted a drag analysis of the vehicle to be performed. Previously, wind tunnel work was carried out for propeller studies. The current investigation uses the results of that work to complete flights for determination of a drag polar for the vehicle. A drag clean-up of the original wing configuration was performed, and though the data are scattered due to the measurement techniques, trends indicate a significant reduction in drag for the new wing. Comparison of the drag data with numerical predictions shows a reasonable correlation.

TABLE OF CONTENTS

LIST OF TABLES

LIST OF FIGURES

ACKNOWLEDGE

I.   INTRODUCTION AND OVERVIEW

The Unmanned Air Vehicle (UAV) is a type of flying vehicle, that is not restricted by the limitations a human pilot. It can be of varing size and purpose and have a large degree of on board autonomy. The mission that can be performed with a UAV is more flexible than with the manned aircraft. The missions which can be performed with a UAV are as follows:

- Surveillance and targeting
- Reconnaissance
- Defense suppression
- Strike
- Electronic warfare
- Communications
- Sensor delivery
- Tactical intelligence
- Assist in search and rescue   [Ref. 1]

In addition, it is possible to use the UAV as a research test bed for other inflight projects. The cost would be lower than the operation of a full-scale manned aircraft.

Many programs are currently using UAV's, both operationally and in flight testing, to obtain the relatively low risk that is only possible through the use of UAV's. In 1986, the Pioneer UAV was selected as the U.S. Navy and Marine Corps Short-Range UAV system. The procurement of a UAV system, once only thought useful as a target drone, marked the beginning of the UAV concept as an important weapon system, worthy of an increased role in U.S. military thinking. The Department of Aeronautics and Astronautics at the Naval Postgraduate School currently has established a UAV flight test program which includes a half-scale Pioneer UAV. The purpose of the overall program is to establish procedures to evaluate vehicle performance of scaled flight vehicles and to investigate methods to improve that performance.

This is a follow-on investigation to the " Development of a Flight Test Methodology for U.S. Navy and Marine Corps Half-Scale Unmanned Air Vehicle " by James C. Tanner [Ref. 2] and "Aerodynamic Analysis of a U.S. Navy and Marine Corps UAV" by Daniel Lyons[Ref. 3]. These previous works by Tanner and Lyons are called hereafter

1

the first-phase work of the half-scale Pioneer flight test. The second-phase investigation includes a completion of the baseline configuration flight test and comparison with the first-phase work. The other flight test was performed with a modified wing. This modified wing configuration includes a smoother wing surface, and an additional sharp trailing edge.

A follow-on investigation will instrument the vehicle to measure control surface deflections, pitch and yaw angles, indicated airspeed, and angular rates and accelerations.

II. FLIGHT TEST PROCEDURE

A. FLIGHT TEST

1. Overview

From the flight test with the half-scale Pioneer, the available data are RPM, ground speed (GS), test weight (W_T) and the basic data of density and temperature. A nondimensional value of propeller advance ratio (J) can be calculated from the following equation:

$$J = \frac{V}{nd} \tag{1}$$

where the V is the true airspeed, n is the flight revolutions per second and the d is the diameter of the propeller. The true airspeed is based upon the averaging of the ground speed as the aircraft flies with and against the wind. The thrust method uses thrust coefficient as a function of advance ratio to determine the aircraft drag in flight.

2. Thrust Method

In level, unaccelerated flight at a given altitude and airspeed, the force equilibrium can be written as shown in Figure 1.
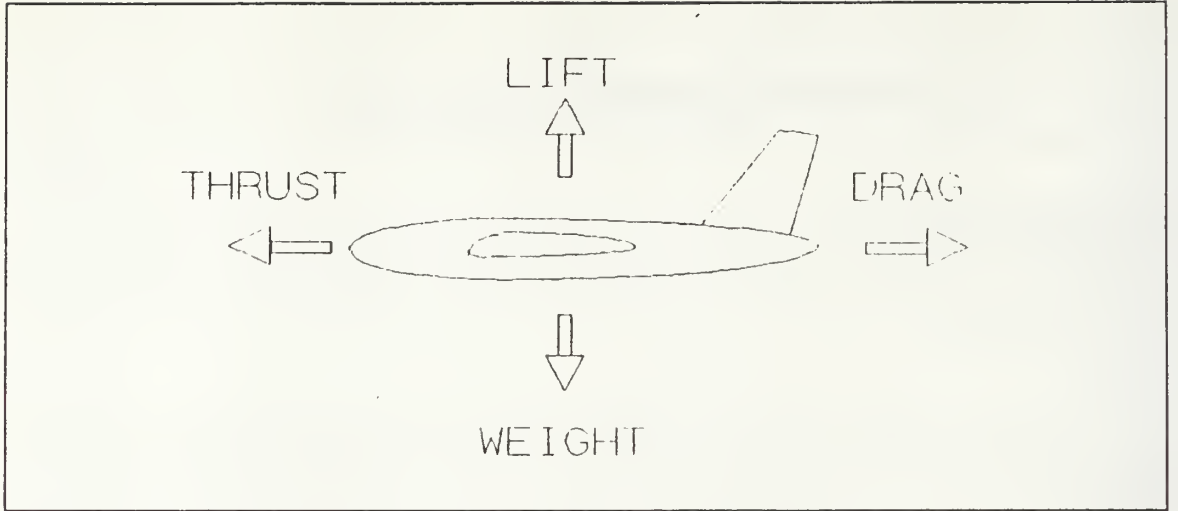
Figure 1.   Force Equilibrium in Level, Unaccelerated Flight.

$$T = D \tag{2}$$

$$L = W \tag{3}$$

From equations (2) and (3), the coefficients are defined as follows:

$$C_D = \frac{2T_E}{\rho_0 V_E^2 S} \tag{4}$$

$$C_L = \frac{2W_T}{\rho_0 V_E^2 S} \tag{5}$$

where ρ_0 is standard sea level density, V_E is the equivalent airspeed, S is the wing area and the W_T is aircraft weight at the test condition. The test weight W_T is obtained using the full fuel gross weight and the weight after landing. The equivalent airspeed V_E can be obtained from the true airspeed, V_T, as follows:

$$V_E = V_T \sigma^{1/2} \tag{6}$$

where V_T is obtained directly from the flight test as will be described, and σ is the density ratio of the test day[Ref. 4].

$$\sigma = \frac{\rho}{\rho_0} \tag{7}$$

4

In order to apply the wind tunnel thrust result from the results of the first-phase work to inflight conditions, the effective thrust T_E is defined as:

$$T_E = C_{T_E} \rho n^2 d^4 \tag{8}$$

where the effective thrust coefficient C_{T_E} can be obtained from the results of wind tunnel testing which was done by Tanner in the first phase of the half-scale Pioneer flight test program as shown in Figure 2 [Ref 2]..
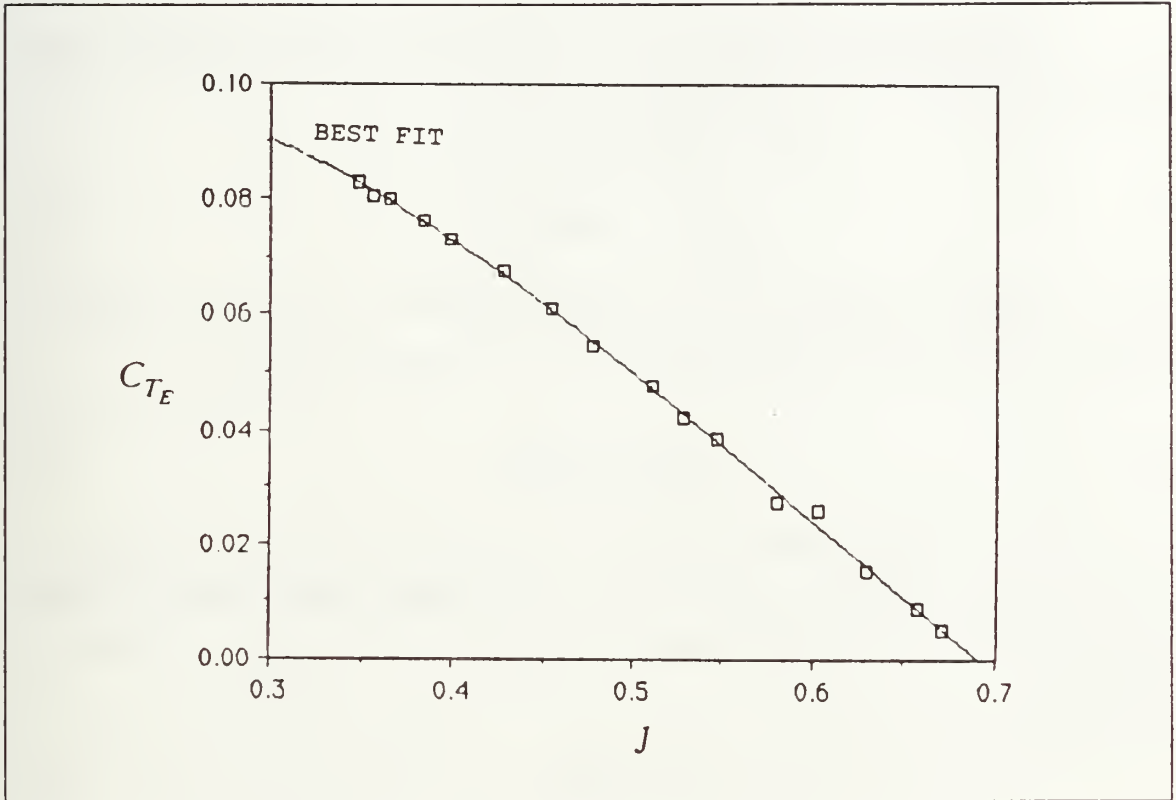
Figure 2.   Effective Thrust Coefficient versus Advance Ratio Plot

The flight test uses the ground course method for airspeed determination. The ground course method is a flight test technique which maintains the heading and the altitude of aircraft from a known fixed position to the another fixed position. If some wind factor exists, then the pilot lets the aircraft drift. The flight test measures the ground speed of the aircraft in two opposite directions of flight. The average of this ground speed is the true airspeed of the aircraft. This relation is expressed as:

$$V_T = \frac{(V_{G_1} - V_W \cos B) - (V_{G_2} + V_W \cos B)}{2} \qquad (9)$$

where V_{G_1} is the ground speed for one direction, V_{G_2} is the ground speed for the opposite direction, V_W is the wind velocity and B is the aircraft's drift angle.

The total drag coefficient(C_D) can then be written as follows:

$$C_D = C_{D_0} + C_{D_i} \qquad (10)$$

where C_{D_0} is the parasite drag coefficient due to viscous forces and C_{D_i} is the induced drag coefficient due to lift. C_{D_i} can also be expressed as:

$$C_{D_i} = \frac{C_L^2}{\pi e AR} \qquad (11)$$

where C_L is the lift coefficient, AR is the aspect ratio and e is the Oswald efficiency factor[Ref. 5: pp. 251-251]. Substituting equation (11) into (10) then gives:

$$C_D = C_{D_0} + \frac{C_L^2}{\pi e AR} \qquad (12)$$

The relationship between C_D and C_L is approximately parabolic such that the C_L versus C_D curve is generally called the drag polar and the relationship between C_D and C_L^2 is a straigt line for which the constant is C_{D_0} and the slope is $\frac{1}{\pi e AR}$. Commonly, it is written as:

$$K = \frac{1}{\pi e AR} \qquad (13)$$

Therefore the total drag coefficient can be written as:

$$C_D = C_{D_0} + K C_L^2 \qquad (14)$$

Since an aircraft can fly at many altitudes over a range of aircraft weights, it is obvious that if the power-required technique is to be used to determine aircraft cruise performance, then a data reduction scheme must be developed to take the flight test data at the various test weights and non-standard atmospheric conditions and reduce them to a standard weight and altitude. The flight test technique used in the United States is called the $P_{iw} - V_{iw}$ method which essentially consists of normalizing the data to an

6

equivalent airspeed and a constant weight, W_s. The normalized power and velocity are expressed as the following equations:

$$V_{iw} = V_T \left(\frac{W_S}{W_T}\right)^{1/2} \sigma^{1/2} \tag{15}$$

$$P_{iw} = \frac{\sigma T V_T}{550} \left(\frac{W_S}{W_T}\right)^{\frac{3}{2}} \sigma^{\frac{1}{2}} \tag{16}$$

The relationship between P_{iw} and V_{iw} are derived by the following procedures:

$$\begin{aligned} P_{iw} &= \frac{\sigma T V_T}{550} = \frac{V}{550}\left(\frac{1}{2}\rho V^2 S C_D\right) \\ &= \frac{\frac{1}{2}\rho V^3 S}{550}\left(C_{D_0} + \frac{C_l^2}{\pi e AR}\right) \\ &= A V^3 + \frac{B}{V} \end{aligned} \tag{17}$$

This can be written as:

$$P_{iw} = A V_{iw}^3 + \frac{B}{V_{iw}} \tag{18}$$

Multiplying both side by V_{iw}, then gives:

$$P_{iw} V_{iw} = A V_{iw}^4 + B \tag{19}$$

The term $P_{iw} V_{iw}$ is linearly related to V_{iw}^4. The slope, A, and the constant, B, are related to the parasite drag coefficient and the Oswald efficiency factor as follows:

$$C_{D_0} = \frac{1100 A}{\rho_0 S} \tag{20}$$

and

$$e = \frac{W_S'^2}{275 \pi AR \rho_0 S B} \tag{21}$$

so,

$$A = \frac{C_{D_0} \rho_0 S}{1100} \tag{22}$$

7

and

$$B = \frac{W_s^2}{275\pi e A R \rho_0 S} \tag{23}$$

[Ref. 6: p.6.3], [Ref. 4].

3. Power Method

Another method to get the drag polar and power-required curve is the power method. The power method was used by Tanner[Ref 2] and includes wind tunnel tests and torque tests. The test shaft brake horsepower, $SBHP_T$, is expressed as:

$$SBHP_T = \frac{2\pi n Q}{550} \tag{24}$$

where Q is the torque from the torque test. The power method uses the propeller efficiency, η, to get the thrust:

$$T = \frac{\eta SBHP}{V_T} \tag{25}$$

where the shaft brake horse power, $SBHP$, is corrected from the standard shaft brake horse power, $SBHP_{STD}$. The standard shaft brake horse power, $SBHP_{STD}$, is corrected using the $SBHP_T$ [Ref. 4]. The propeller efficiency, η can be plotted with the advance ratio, J, as shown in Figure 3.
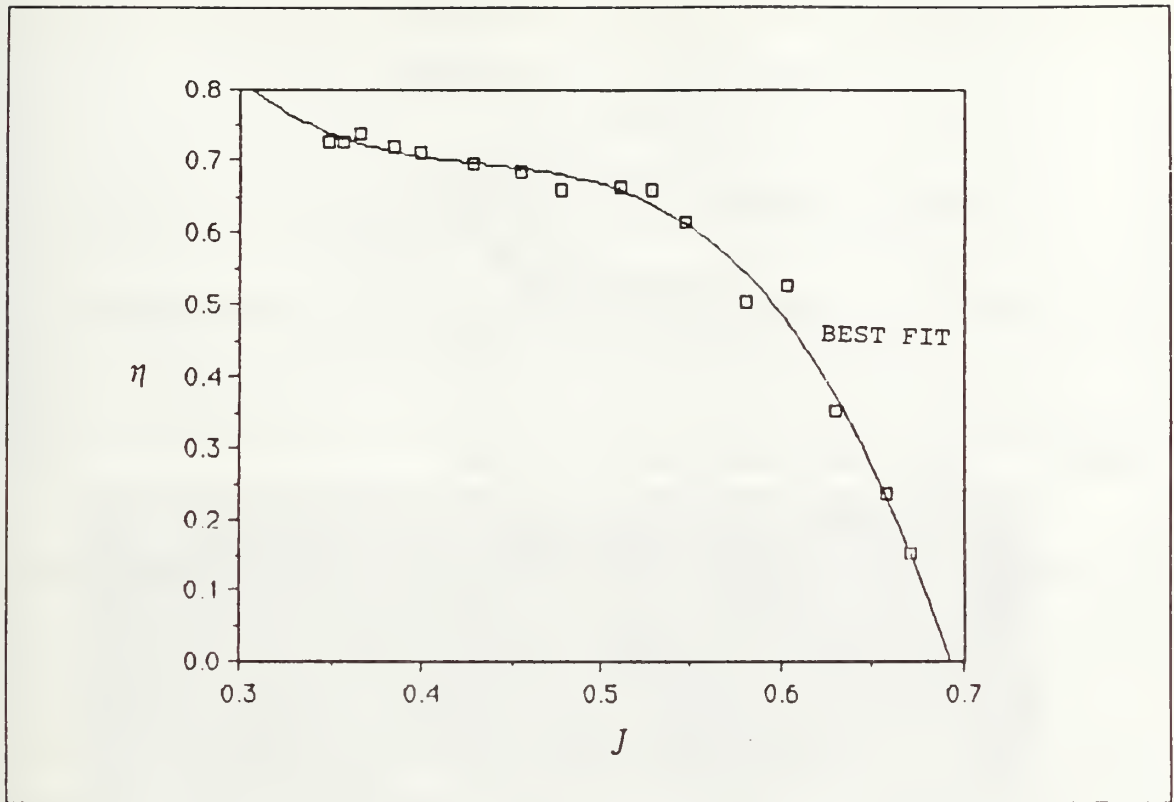
Figure 3.   Propeller Efficiency Versus Advance Ratio

The power method would require identical throttle settings for the aircraft and the engine on the torque stand. Due to the difficulty of maintaining exact correlation of throttle settings, the thrust method was preferred.

B.   DRAG ANALYSIS

Considering the flow past a solid i.e. a wing, the velocity of the flow at the surface is zero because of friction between the fluid and the solid material. There is also a thin region of retarded flow in the vicinity of the surface as sketched in Figure 4.
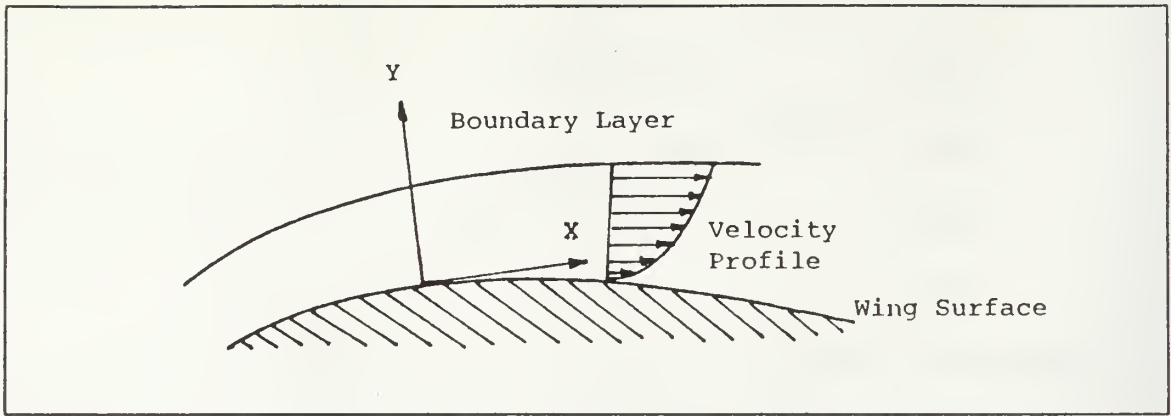
Figure 4.   Flow With Friction Over Wing Section

This region of viscous flow which has been retarded due to friction at the solid surface is called a boundary layer[Ref. 5]. Within this boundary layer, two types of flows exist: laminar flow and turbulent flow. Both flows are a function of Reynolds number which is a function of the distance along the airfoil's surface x and the dynamic viscosity. Laminar flow exists from the leading edge of the airfoil to a chordwise point on the surface corresponding to a Reynolds number ranging from 10,000 to 500,000. Laminar flow is characterized by a flow that is mostly uniform and has a relatively low inertia drag. Turbulent flow is characterized by a great deal of fluid mixing and unsteady motion. This flow has a relatively high drag due to inertia effects.

The transition location from a laminar to a turbulent boundary layer is difficult to predict accurately. This prediction is particularly difficult at Reynolds numbers below 1 million. The full-scale Pioneer operates at a Reynolds number of approximately 1,350,000, while the half-scale Pioneer operates at a Reynolds number of 500,000. At these relatively low Reynolds numbers, the boundary layer behavior can be sensitive to freestream disturbances, surface imperfections, and contour inequalities. The surface of the wing of both vehicles is currently a flat painted finish applied to the exposed weave of the fiberglass. As the Pioneer has failed to meet its endurance prediction, ways to easily reduce the aircraft drag are being considered. It is desired to know whether the drag of the wing is being penalized by the surface condition. Also, the half-scale wing is configured with a blunt trailing edge. It is desired to know whether a more complete airfoil contour may be beneficial in improving the lift- to-drag behavior of the wing, as measured by flight test of the vehicle.

10

III. EXPERIMENTAL EQUIPMENT

A. GENERAL CONFIGURATION OF THE HALF-SCALE PIONEER

The half-scale Pioneer is an unmanned air vehicle which is currently being used by the Navy and Marine Corps for training. The half-scale Pioneer is a twin boom tail(twin vertical stabilizer and rudder), pusher-type aircraft as shown in Figure 5.
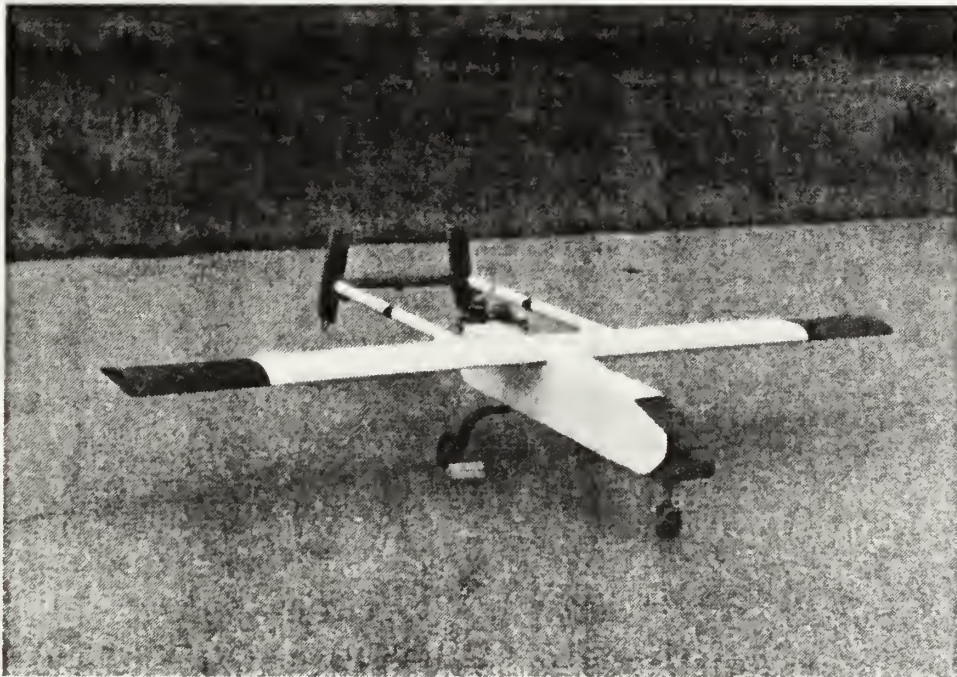
Figure 5.   Half-Scale Pioneer

The aircraft has a wing span of 8.19 feet, a chord of 0.91 feet and an aspect ratio of 9.03. The rectangular wing consists of an Clark Y airfoil with no sweep, dihedral or twist. The fuselage has a trapezoidal cross-sectional area of 0.29 square feet and is 4.17 feet long. The twin-boom tail which is constructed of 1-inch diameter aluminum tubing, is 2.67 feet long and supports the horizontal stabilizer. The overall length of the aircraft

11

is 5.29 feet. A 3-D view of the half-scale Pioneer is shown in Figure 6 and a specification summary is listed in Table 1 on page 13.
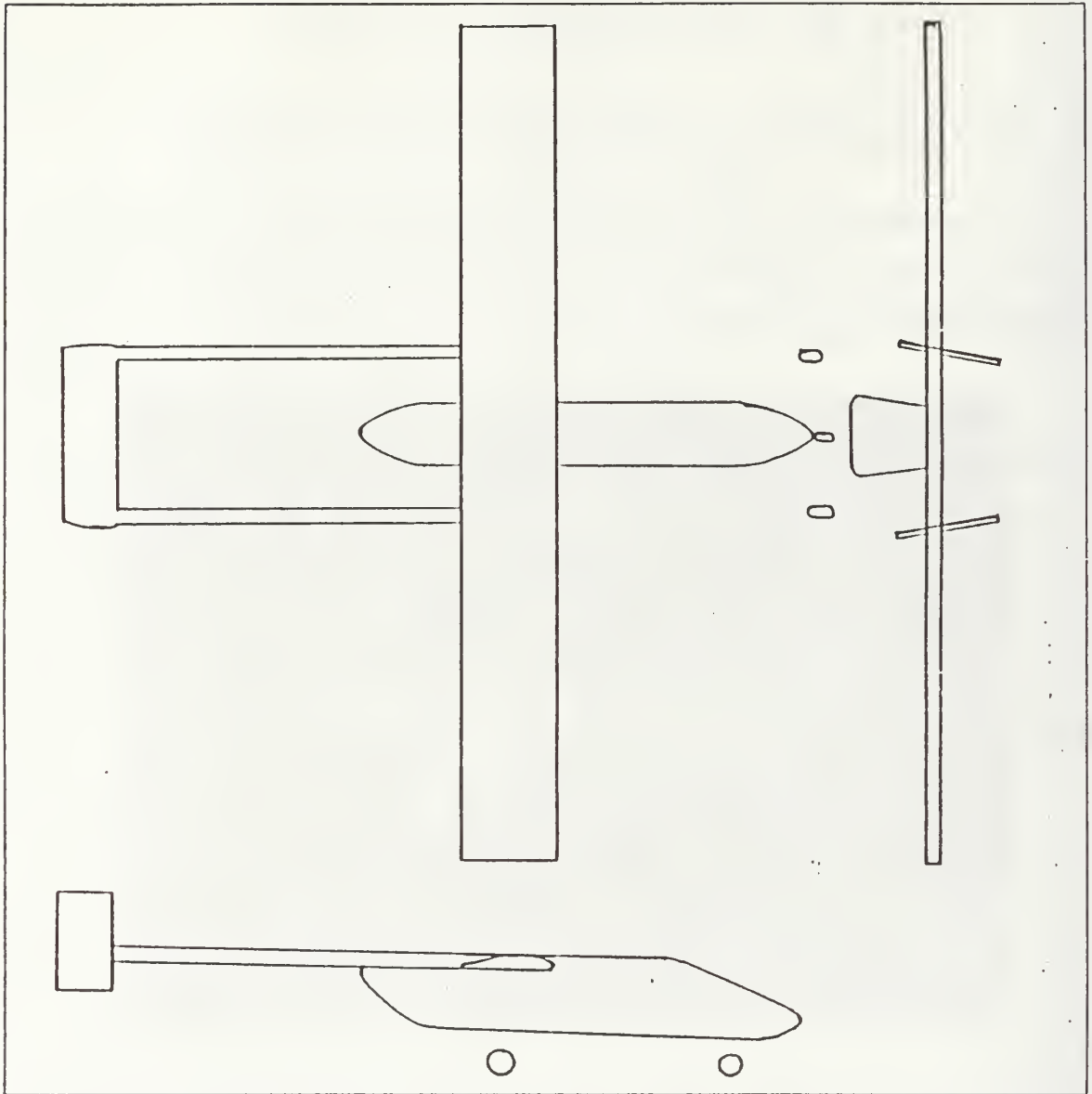
Figure 6.   3-D view of Half-Scale Pioneer

Table 1.   ORIGINAL HALF-SCALE PIONEER SPECIFICATION SUMMARY

Total Length	5.92 FT
Fuselage Length	4.17 FT
Wing Span	8.19 FT
Wing Area	7.453 FT^2
Wing Chord	0.91 FT
Wing Aspect Ratio	9.03
Gross Weight	28.00 LBS
Wing Loading	3.76 LBS/FT^2
C.G. Location	33 % C_{MAC}
Horizontal Tail Span	1.53 FT
Horizontal Tail Chord	0.50 FT
Horizontal Tail Area	5.92 FT
Horizontal Tail Aspect Ratio	3.06 FT
HOrizontal Tail Volume	2.34 FT^3
Vertical Tail Span	1.01 FT
Vertical Tail Chord	0.50 FT
Vertical Tail Area(2)	1.01 FT^2
Vertical Tail Aspect Ratio(1)	2.02 FT
Vertical Tail Volume	3.09 FT^3

The half-scale Pioneer is constructed primarily of fiberglass with quarter-inch plywood bulkheads and support ribs. There are three access panels on the body for assembling and maintanence. The subassemblies are the main wing, tail boom and body. In the fuselage are located the radio receiver, pitch and roll rate gyros, nose wheel steering servo and engine throttle control servo. The engine is mounted at the rear of the fuselage and employs a pusher-type propeller. In addition, a magnetic sensor is installed in front of the propeller and a tape recorder is installed on the gyro control box for recording inflight RPM data. An 18-ounce capacity fuel tank is installed at the center of gravity position which is located at 33 percent of mean aerodynamic chord (C_{MAC}). In the main wing there are two servos which control aileron deflection. The empennage requires three servos, which include one elevator servo and two rudder servos.

B.   CONTROL SYSTEM

The half-scale Pioneer has a control system with a 8-channel radio transmitter, receiver, two rate gyros, seven servos and 4.8 VDC battery pack. The transmitter uses a pulse-coded modulated signal which provides increased signal reliability. The transmitter was also equipped with an optical tachometer wand to measure propeller RPM to ± 100 RPM for a ground check. The rate gyros were mounted on the aircraft longitudinal C.G. position and were used to help stabilize the aircraft pitch and roll axes during flight testing and to reduce the pilot's work load. Figure 7 shows the electronic gear layout used in this investigation [Ref. 2].
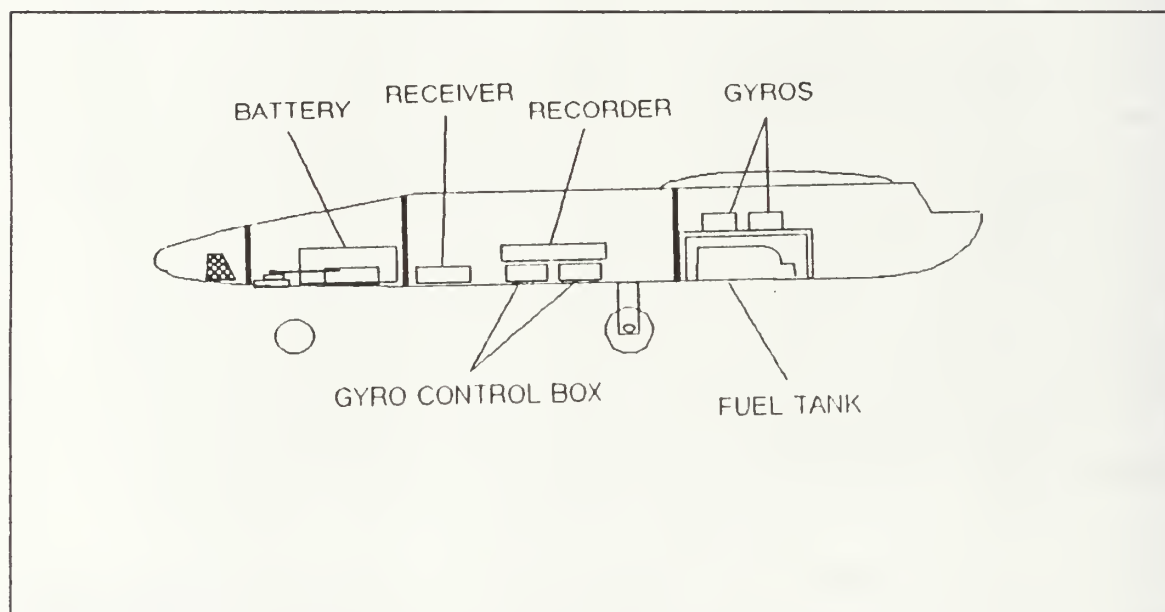
Figure 7.   Half-Scale Pioneer Equipment Layout in Body

The nose wheel steering and engine throttle servos were installed inside of the body. The remaining servos were installed near their respective control surfaces in order to reduce the length of the control linkage. The rudder control servos and nose wheel control servo are connected with Y-type cable connectors such that they respond to the same control input. The two rudder control servos are installed such that one servo serves as the master and the other serves as the slave.

14

C. PROPULSION SYSTEM

The half-scale Pioneer is equipped with a two-stroke glow plug engine. A muffler is used to reduce the noise of the engine. The engine has a 1.088 cubic-inch displacement and is rated at 3 HP at 16000 RPM. The engine RPM range is from 2000 to 16000 RPM as specified in the manufacturer's manual. A 14-inch diameter, 6-inch pitch pusher-type (14x6P) propeller is installed on this engine. For the engine fuel supply, an 18-ounce fuel tank was installed near the center of gravity of the aircraft to minimize the C.G. movement during flight as shown in Figure 7. A fuel pump to feed fuel to the engine is required because the engine is placed 5 inches above the fuel tank. The engine fuel consumption could be calculated by checking the flight time and the remaining fuel in the tank. In this investigation the fuel consumption was determined to be 0.05 pounds per 1 circuit of 1500 feet, which was determined empirically in the first-phase.

D. DATA COLLECTING SYSTEM

1. Onboard System

A magnetic proximity sensor was installed on the aircraft radial engine mount as shown in Figure 8. Two steel posts, 0.125 inches in diameter and 0.75 inches in length, were mounted 180 degrees apart in the engine drive washer to give a signal to the magnetic sensor.

A small tape recorder was used for recording the inflight propeller RPM. The recorder used a high-quality tape coated with C_iO_2 for the precise signal recording.
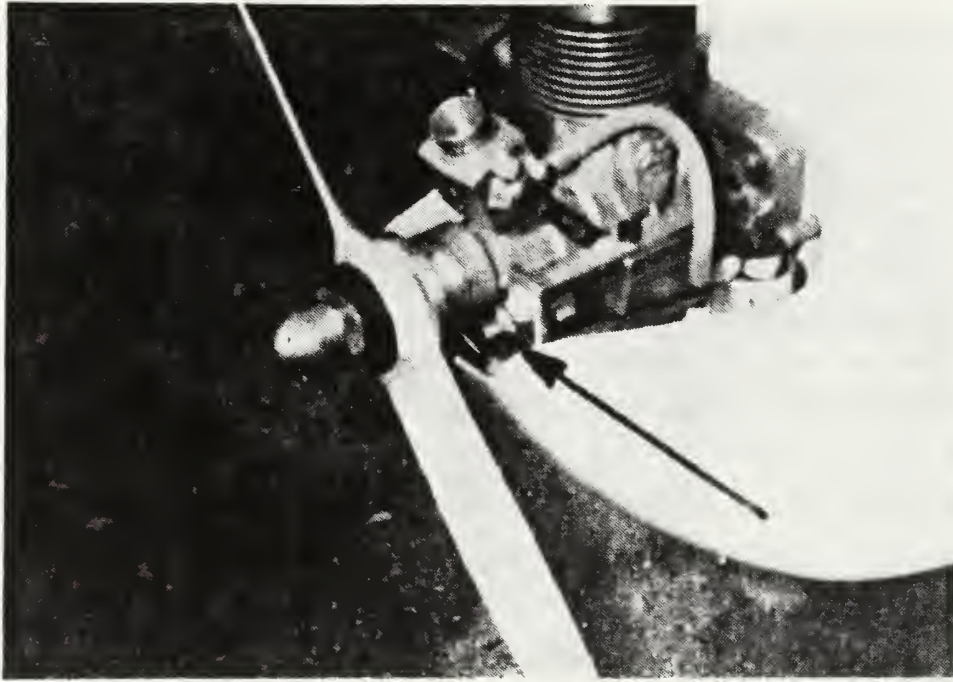
Figure 8.   Minarik PK-1 Magnetic Proximity Sensor Mounted on Engine

2.   Ground Data Reduction System

The signal from the tape recorder was conditioned through a signal conditioning wave shaper to remove the noise and to provide a clean signal for the frequency counter. The signal conditioning wave shaper is shown in Figure 9.
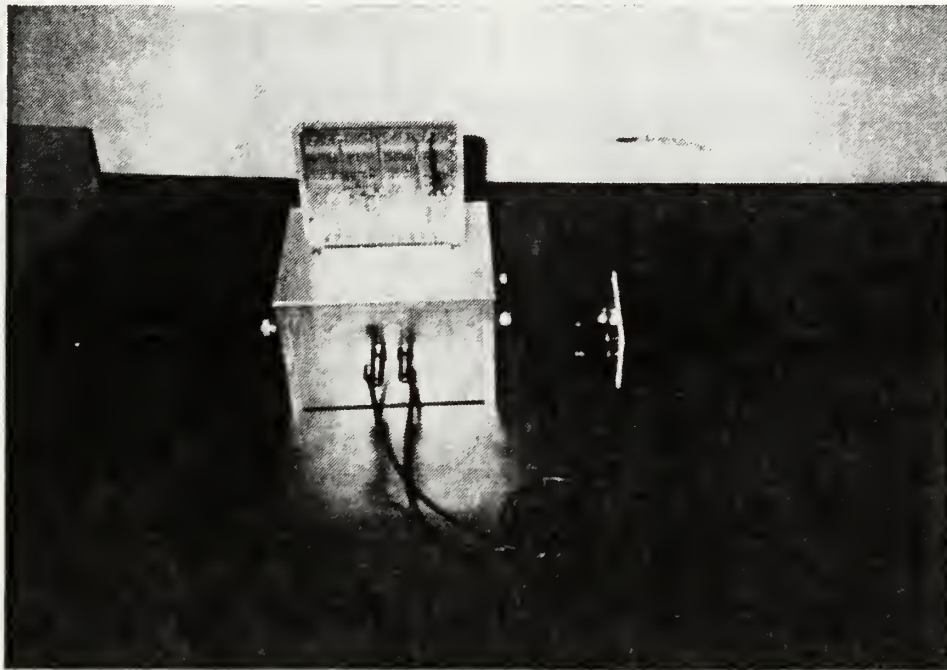
Figure 9.   Signal Conditioning Wave Shaper

E.   CONFIGURATION CHANGED FROM FIRST PHASE

Some changes of aircraft configuration were made with respect to equipment position, weight and landing gear mechanisms. In the previous flight tests, there were two problems associated with the aircraft landing gear. Originally, the wheels were made of hard rubber which had no shock absorption. Also the main gear and nose gear struts were made of fiberglass which has little shock absorbing properties. Additionally, the C-shaped nose wheel strut acted as a spring causing the aircraft to porpoise if the landing operation was not properly controlled. Figure 10 shows the original landing gear system in the first phase.

17
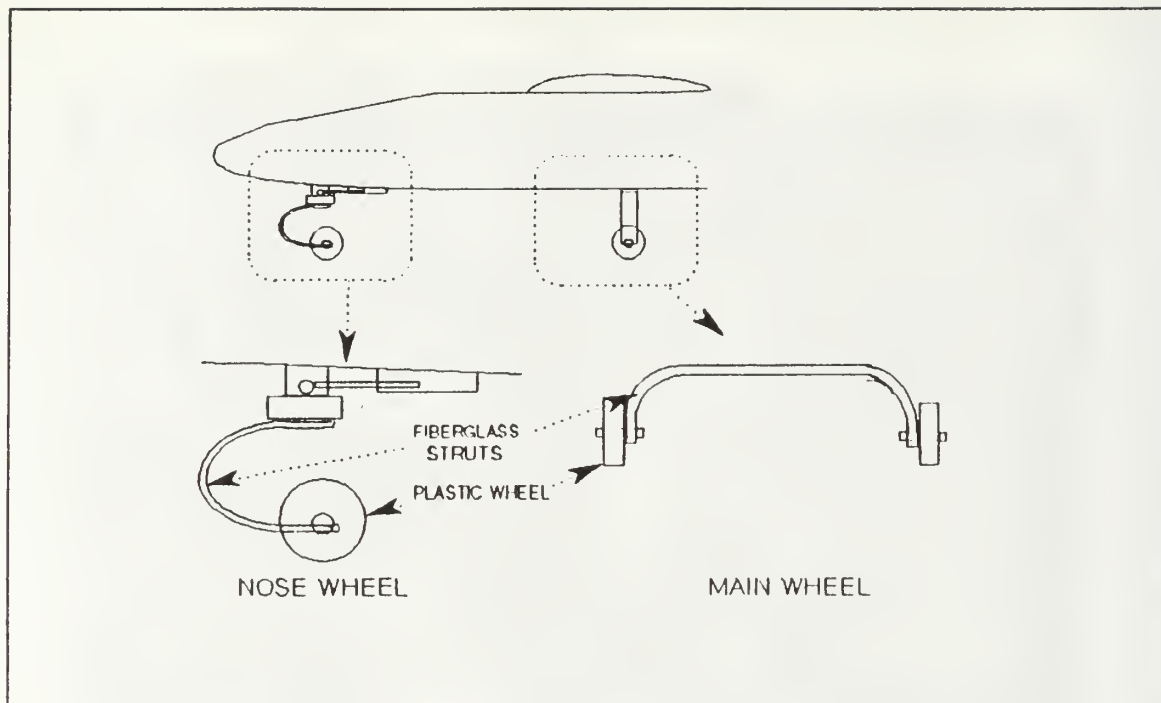
Figure 10.   Original Landing Gear System in First Phase

During the flights in the first-phase, the nose gear strut was sheared as a result of the landing gear problems. A second accident occurred during a landing in the first-phase of flight testing in which the front of the fuselage, where the nose gear is connected, ruptured.   Due to these experiences, the nose wheel strut was redesigned to include damping shock absorbers and soft tires were substituted. With redesigning the gear system, the frontal area is equivalent to the original half-scale Pioneer as shown in Figure 11.

18
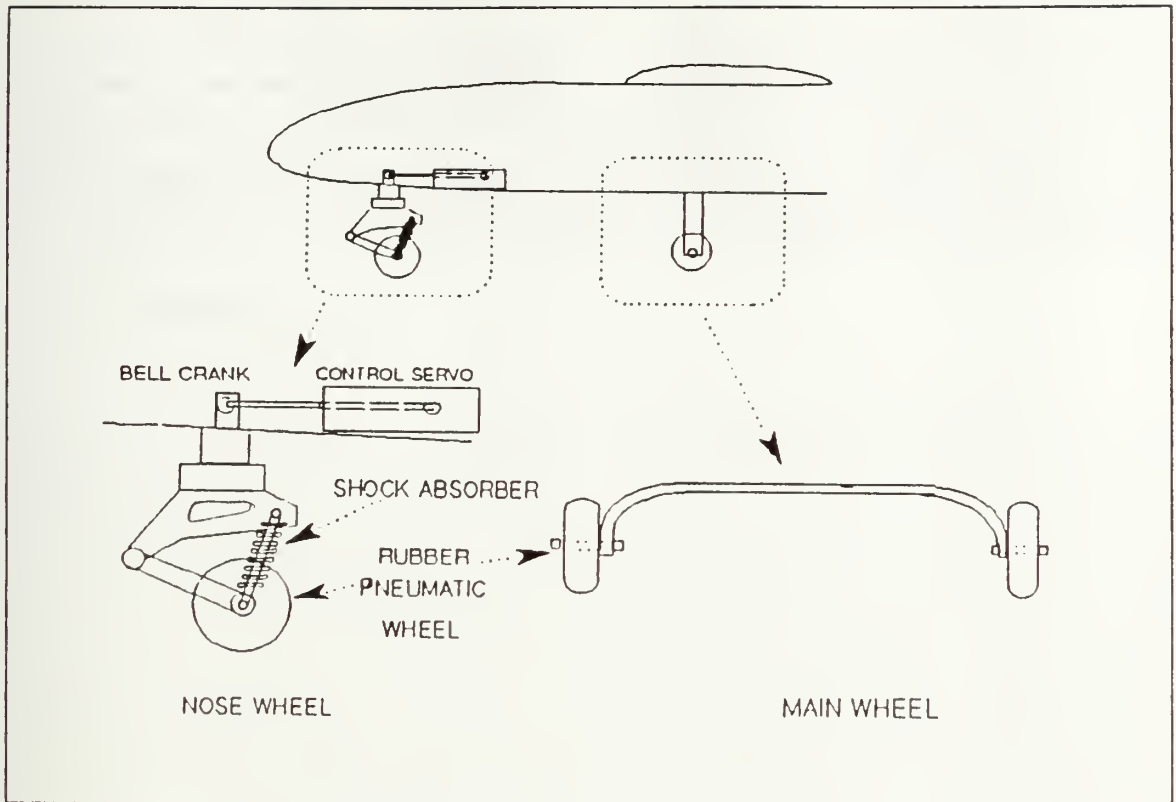
Figure 11. Changed Landing Gear System Configuration

A comparison of the frontal area of the three landing gear between first case and second case is listed in Table 2.

Table 2.   FRONTAL AREA CHANGE COMPARISON

		1st Phase	2nd Phase
Frontal Area (in^2)	Nose Gear	12.72	11.35
	Main Gear	2.65	4.37
Total Area		15.37	15.72

The nose gear servo, originally located outside of the fuselage, was placed inside to eliminate external drag. Therefore, more room for the nose wheel steering control system was needed. The ballast weight was moved further forward and the battery was relocated at the front body wall to keep it from interupting the nose wheel steering control. The recorder was moved further aft to the same location as the rate gyros. As a result of the

component movement. 0.7 pounds of ballast weight were removed for the purpose of maintaining the aircraft center of gravity at 33 percent of C_{MAC}. This reconfiguration only changed the entire aircraft weight by less than 1 percent and therefore can be considered as the same configuration as the original aircraft. The following investigation is based on the assumption that the configuration of the modified aircraft is equivalent to the aircraft used in the first-phase.

IV. EXPERIMENTAL PROCEDURE

A. FLIGHT TEST WITH UNMODIFIED WING SURFACE

1. Preflight Preparation

The day before each flight test, the aircraft was readied for flight. The transmitter battery and aircraft battery pack were recharged and the test instrumentation was installed and checked to insure proper working order. The aircraft weight was checked with full fuel, which was used to determine the test weight, W_T. The aircraft center of gravity was adjusted using the weight in the nose of the aircraft to ensure that the C.G. was at 33 percent C_{MAC} as recommended by the Pioneer's manufacturer. There are two methods to check the center of gravity. The first one is to measure the weight on each wheel and using the moment equilibrium equation from a fixed point, solve the equation for the C.G. position. The dimensions needed for calculating the center of gravity are shown in Figure 12. The other method is to lift the aircraft at the wing tips to locate the C.G. position. This method is commonly used by aircraft modelers.

STATION NO.	DISTANCE FROM #0
1	6.00˝
2	26.24˝
3	33.40˝
4	37.38˝ (38.2˝)
5	51.95˝
6	65.04˝
7	71.04˝
	( ) Modified Wing
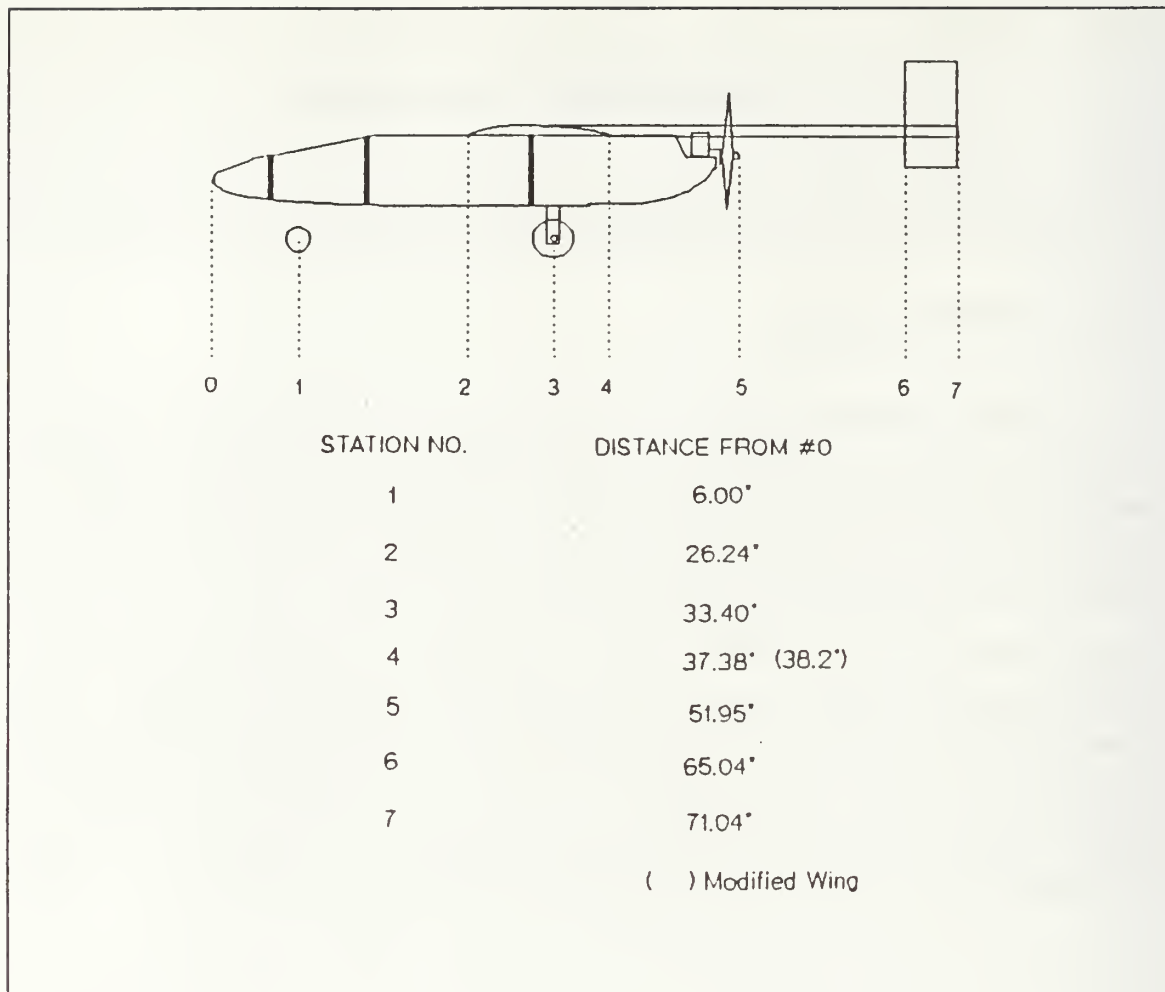
Figure 12.   Dimensions for Calculation of C.G.

2.   Flight Test at Airfield

Flight testing was conducted at Fritzsche Army Airfield, Fort Ord, CA. The aircraft was disassembled into the three subassemblies for transport to the airfield. At the airfield these parts were reassembled for flight, then a preflight was performed to check all of the components for proper operation.

After the preflight and radio check, the aircraft was flown through a sequence of touch and goes to provide the pilot with warm-up flight time as well as to check the aircraft control characteristics and the trim setting of the radio transmitter. Once the

aircraft was landed and refueled, the onboard recorder was switched on to begin recording the engine RPM.

The flight tests required at least four people to perform the data recording tasks. During the flight, two men stood at a fixed distance 1500 feet apart along the air field runway and when the aircraft passed directly over each man's head, that man then gave a "hack" signal to a person recording data standing next to the pilot. In this manner, ground course speeds were timed for determination of airspeed for the different throttle settings. The positions of these people, the aircraft flight route and field distance are shown in Figure 13.
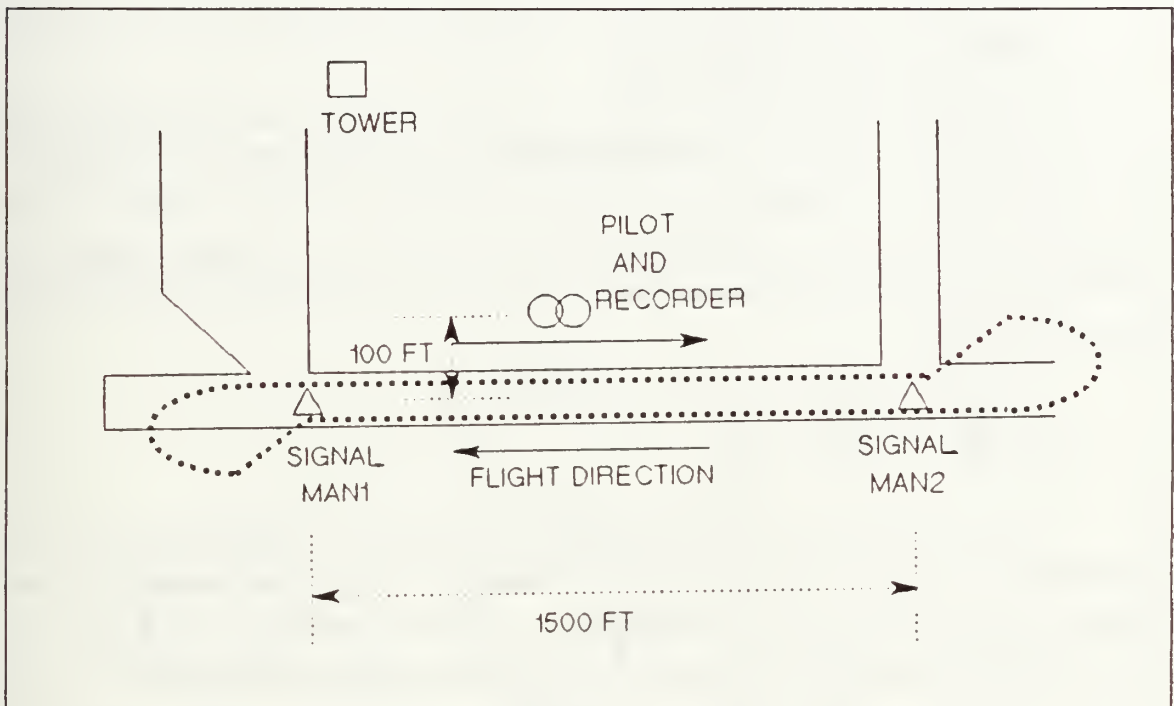
Figure 13.   Position of Man and Flight Route of the UAV Flight

When the signal man gave the hack sign, the recorder recorded the time of flight to fly in a specified direction of 1500 feet. After one period of flight, the amount of fuel remaining in fuel tank was checked to determine the flight test weight during the runs.

Flight testing was conducted over the complete airspeed range in level flight. Due to the lack of an onboard pilot, it is hard to maintain an exact aircraft heading and altitude. The radio control pilot can only control by watching the aircraft from a long distance. As a result, the airspeed is difficult to control. The ground course method to determine the airspeed is relatively simple. Even though a wind factor exists, the error

due to the headwind is removed because the headwind factor is canceled out automatically as discussed in Chapter II. An attempt was made to allow the airplane to drift along the runway heading. However, it was found to be difficult to maintain the runway heading by eye, so usually the pilot held the runway track, causing an error due to crosswind. The error was small, because the ratio of the crosswind and the airspeed of the aircraft is small. For example, if there exists a 5 knot crosswind then the ground speed error was less than 1 % by simple vector calculation. The half-scale Pioneer has limited controllability in strong cross winds during the landing phase. Therefore, flight testing was completed in the morning during low winds.

Also, the wind direction and velocity, temperature and pressure were measured using portable measuring instrumentation.

In the first phase, the half-scale Pioneer was tested with an unmodified wing which had a rough surface with exposed fiberglass weave and a blunt trailing edge. The results from the first-phase flight tests are listed in Appendix A. There is insufficient data to obtain good results for a drag polar as shown in Figure 22. Therefore, flight tests with the unchanged wing were conducted to obtain data points not obtained during the first phase of work.

3. Data Reduction

After the flight test, recorded frequency data on the onboard tape recorder was correlated with the flight time over the 1500-foot distance test. An oscilloscope was used to examine the output signal of the recorder and signal conditioning wave shaper. The signal conditioning wave shaper was used to get an amplified rectangular pulse from the saw tooth electrical pulse as shown in Figure 14. The conditioned output signal was more clearly counted by the frequency counter. A frequency counter was then used to get the frequency of revolution of the propeller.

(a) Unconditioned Signal   (b) Conditioned Signal
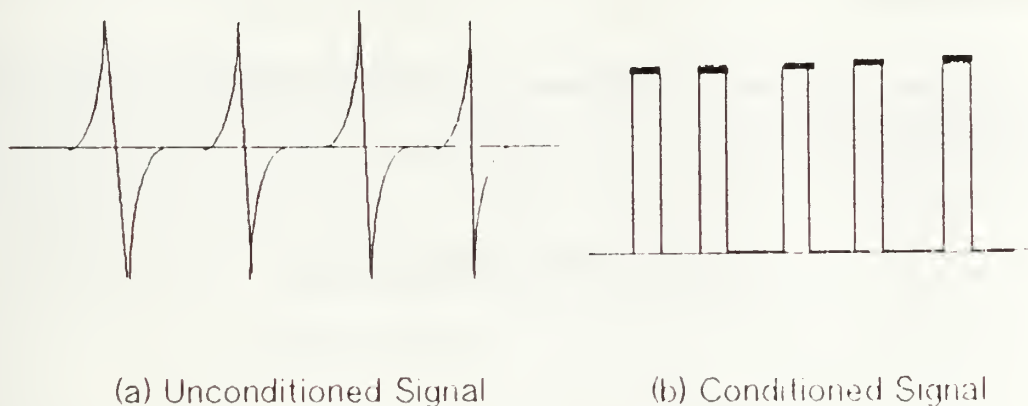
Figure 14.   The Results of Signal Conditioning

The signal conditioning network is shown in Figure 15.
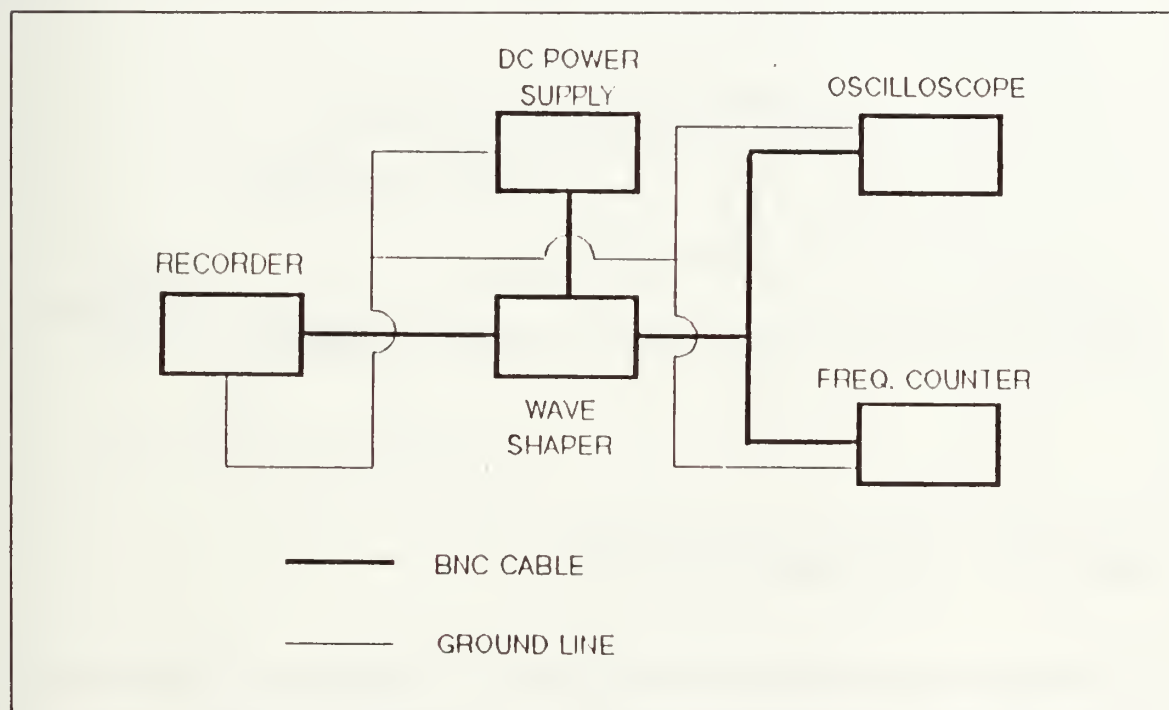
Figure 15.   The Network For Signal Conditioning

B. FLIGHT TEST WITH A SMOOTHER WING SURFACE AND MODIFIED TRAILING EDGE

In this step, the aircraft wing surface was smoothed and a sharp trailing edge was added as shown in Figure 16.
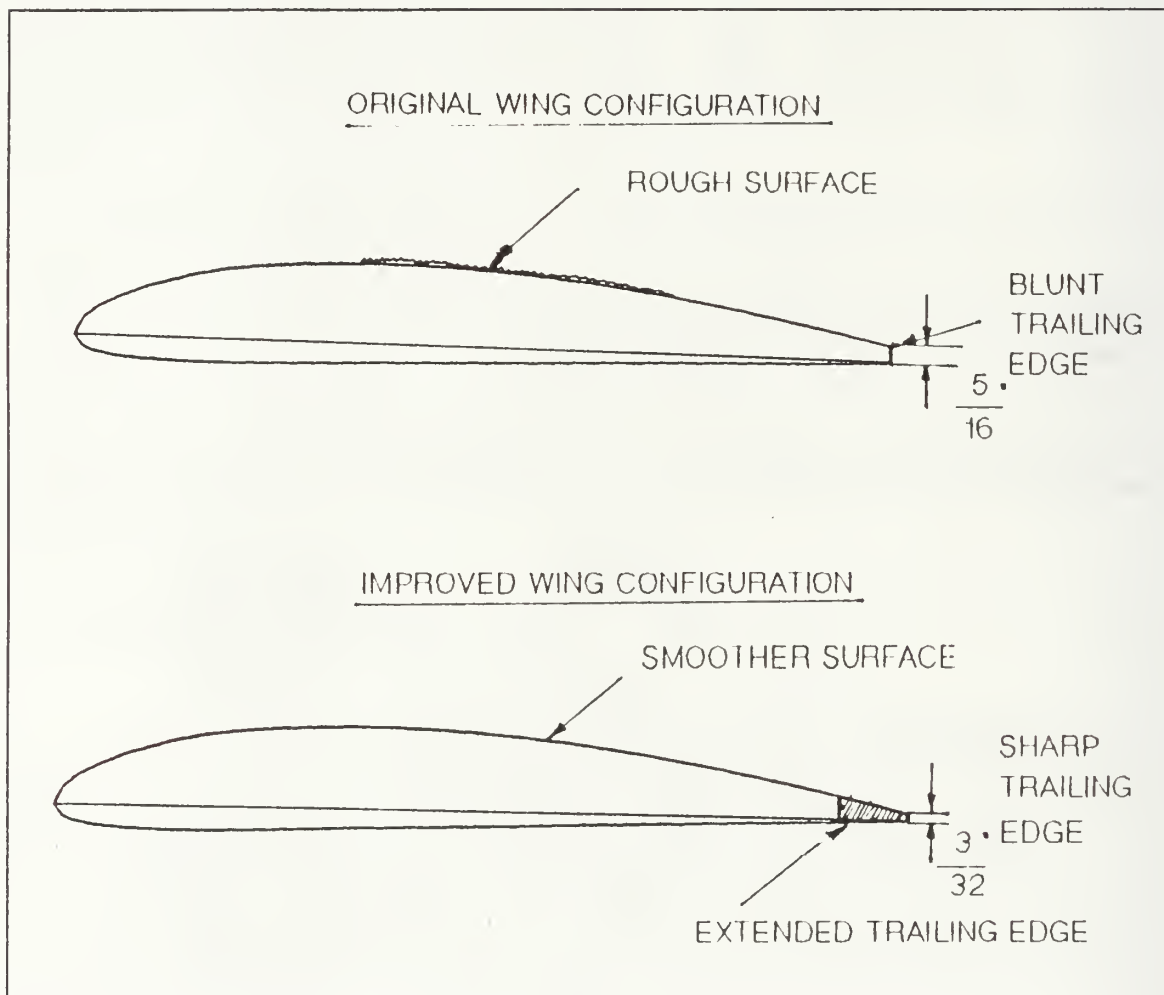
Figure 16.   Wing Configuration Changes

A smoother wing implies that the flow around the wing surface should be laminar for a greater distance along the wing chord than the original wing surface. Therefore in this step of the experiment, the wing surface had to be refinished carefully. Also, the trailing edge of the wing was changed to obtain a sharp edge. As a result of modifying the wing surface and the trailing edge, the chord of the wing became 9 % greater than

the original wing, the aspect ratio changed to 8.26, and the wing surface area increased to 8.122 square feet. These changes in the wing are listed in Table 3 on page 27.

Table 3.   WING CONFIGURATION CHANGES COMPARISON TABLE

CHANGED ITEM	ORIGINAL	MODIFIED
CHORD	0.91 ft	0.99 ft
ASPECT RATIO	9.03	8.26
WING AREA	7.453 ft^2	8.122 ft^2

V. RESULTS AND DISCUSSIONS

Flight tests were performed with two kinds of wing configurations. One is for the supplimentary flight test of the first-phase work and the other is for the modified wing configuration.

A. FLIGHT TEST RESULTS WITH ORIGINAL WING CONFIGURATION

Supplimentary flight test raw data are listed in Table 11 on page 48and in Table 12 on page 49 in Appendix B. The data for the aircraft characteristics of the original configuration are listed in Table 13 on page 50, Table 14 on page 51, Table 15 on page 52 and Table 16 on page 53 in Appendix B. The half-scale Pioneer drag-polar for the original configuration is shown in Figure 17. The solid line curve fit came from the equation generated from the linear regression plot of C_D versus C_L^2 as shown in Figure 18. The dotted line shows a predicted curve which was made by Lyons in the first-phase. The data for the predicted curve is listed in Table 10 on page 46 in Appendix A. It is seen that the actual drag values are higher than predicted, though the induced drag appears to be fairly well predicted. From the slope and Y-intercept of the linear regression equation, the C_{D_0} and e for original wing configuration were determined to be 0.069 and 0.22 respectively. These values are compared to the results of the first-phase work in Table 4 on page 31.
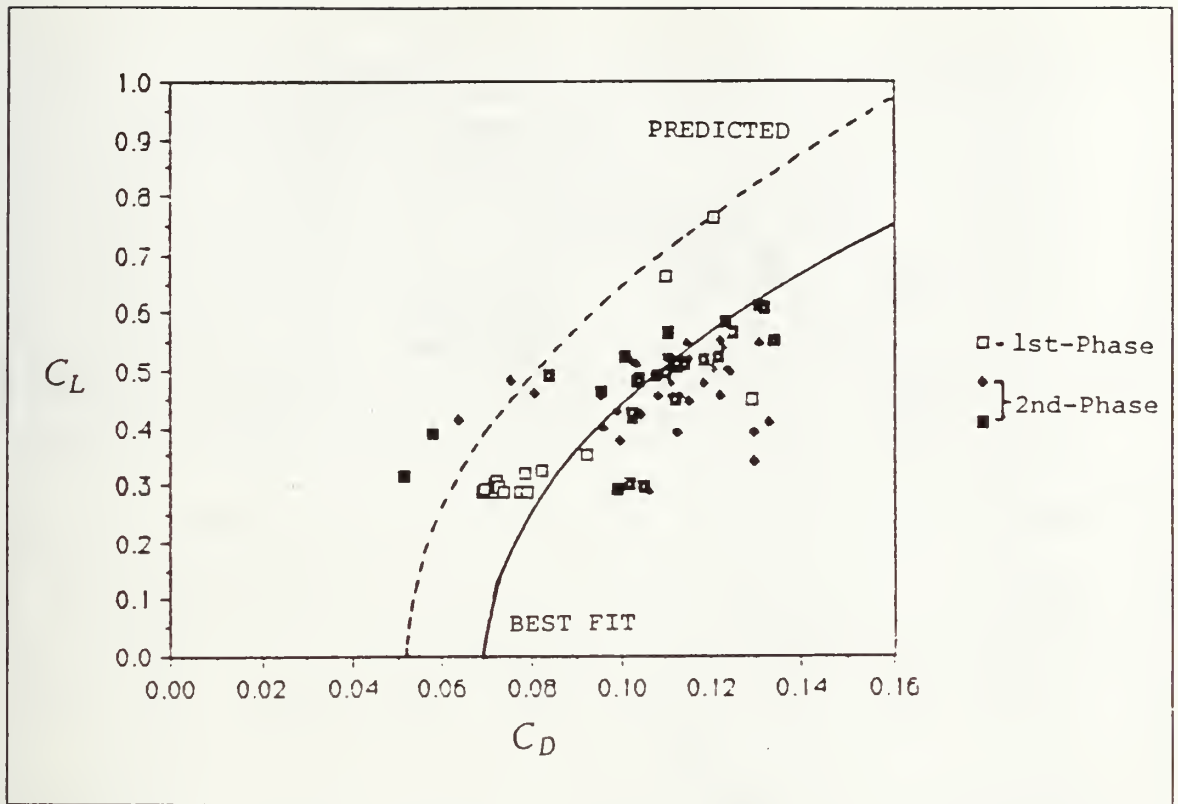
Figure 17.   Drag Polar For Original Wing Configuration
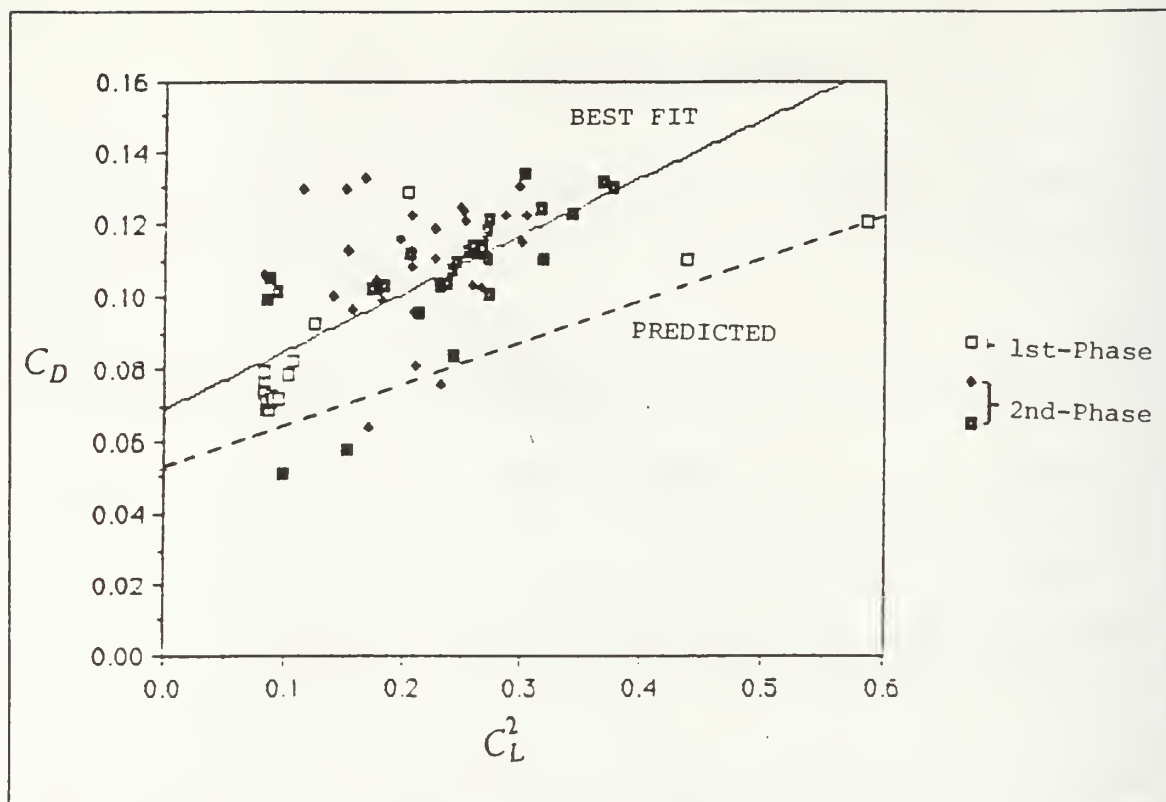
Figure 18. Drag Polar Linear Regression For Original Wing Configuration

The power required data were standardized using the $P_{iw} - V_{iw}$ method. The power-required curve is shown in Figure 19. The solid line curve fit through these data points was carried out by plotting the equation of the line generated from the $P_{iw}V_{iw}$ versus V_{iw}^3 linear regression plot shown in Figure 20. This method is a standard flight test data analysis reduction technique. The Oswald efficiency factor, e, and C_{D_0} for this method were determined using the constants generated from the linear regression and were 0.0808 and 0.235 respectively. The P_{iw} versus V_{iw} plot also estimated the velocity for maximum endurance of 50 ft/sec and a maximum range velocity of 60 ft/sec. These values are compared with the result of the first-phase work in Table 4 on page 31.

30

Table 4.   CHARACTERISTIC COMPARISON BETWEEN 1ST-PHASE AND 2ND-PHASE

	1st-Phase	2nd-Phase	Method
C_{D_0}	0.0697	0.0691	Drag-Polar
e	0.371	0.220	Drag-Polar
C_{D_0}	0.0621	0.808	$P_{iw} - V_{iw}$
e	0.197	0.235	$P_{iw} - V_{iw}$
V_{maxR}	70 ft/sec	60 ft/sec	$P_{iw} - V_{iw}$
V_{maxF}	55 ft/sec	50 ft/sec	$P_{iw} - V_{iw}$
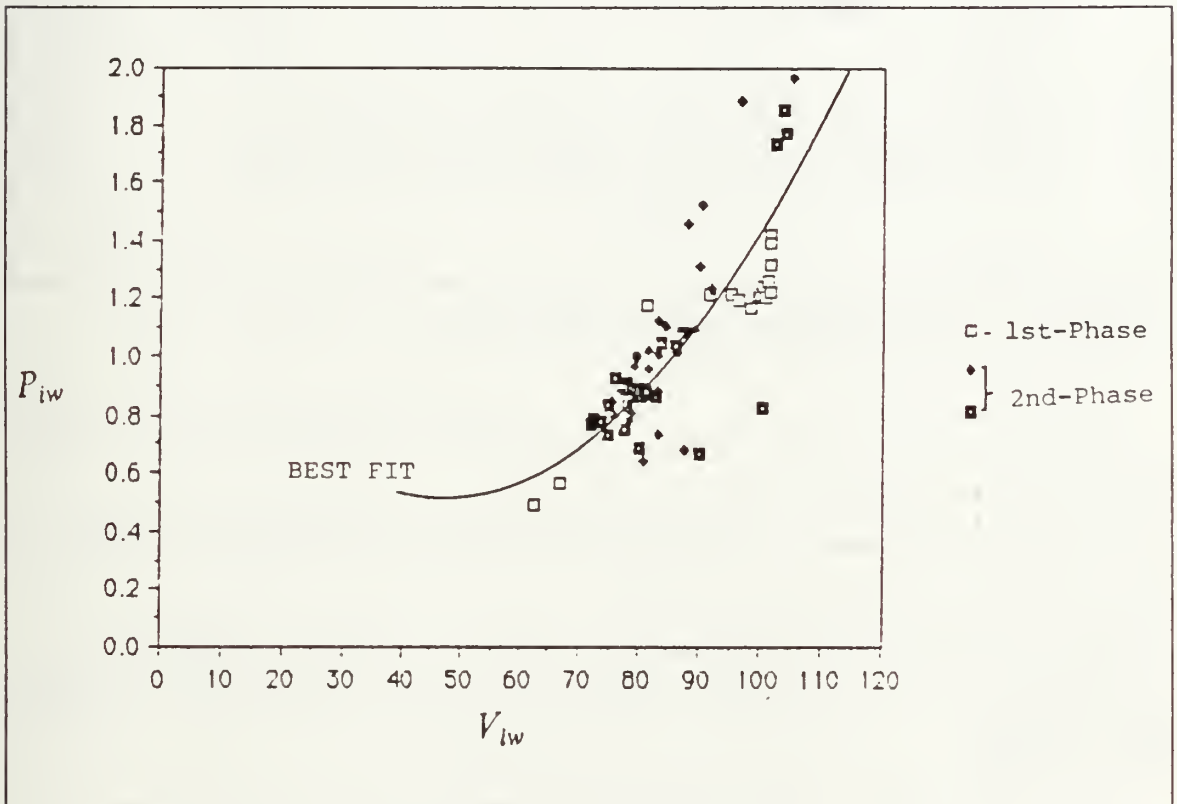
Figure 19.   Piw Versus Viw Curve

31
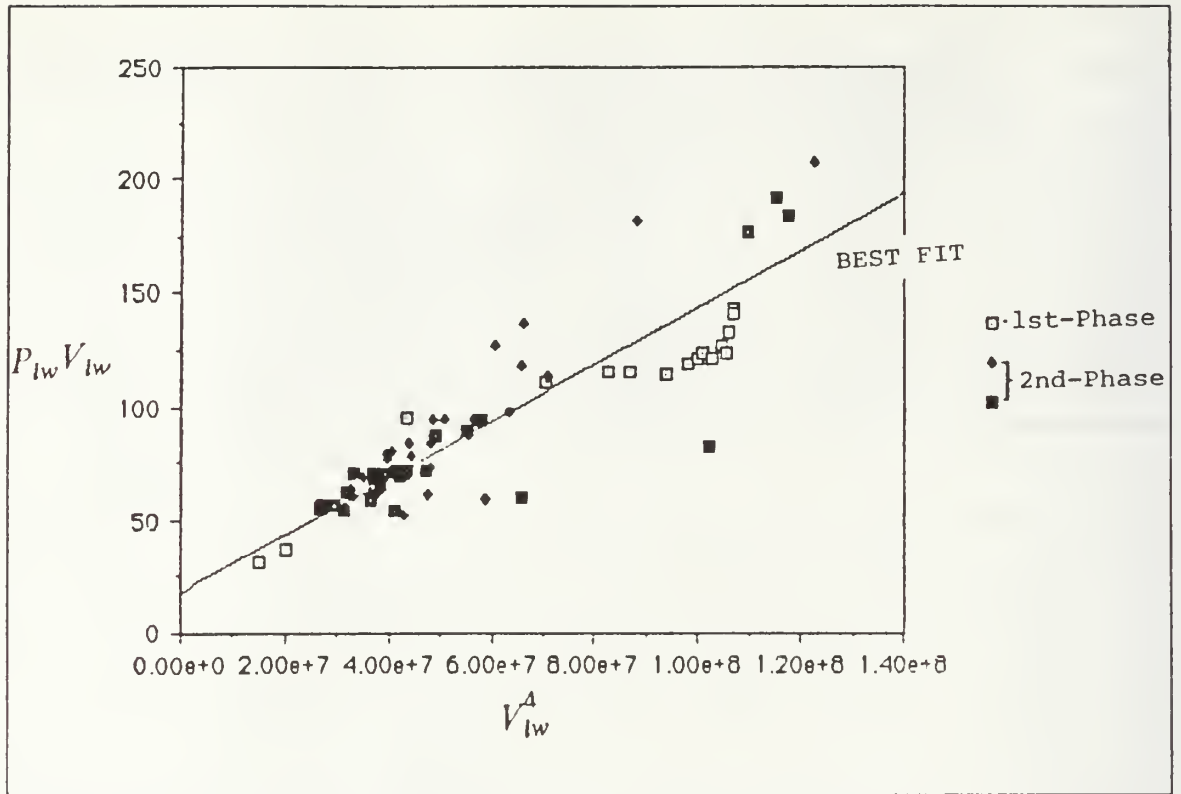
Figure 20.   Power Required Linear Regression Plot

Comparing the drag-polar and power-required curves to the results of the first-phase work, the second-phase work shows similar trends. Numerically, the C_{D_0} is almost same as the result of first-phase work in the thrust method. As the result of the first-phase work, the result of the supplimental flight test turned out to be a higher drag than the predicted drag. The higher drag might comes from the skin friction drag due to the exposed fiberglass weave and the blunt trailing edge. Therefore, the improved wing flight test was needed.

Also, the distribution of the data points in the above plot is largely scattered. The scattered distribution would be related to the error of the flight. There are several factors that could be a source of error in the UAV flight testing, including human timing error due to the signal man and observer, aircraft flight path error due to altitude change and course change, and cross wind error. Also, a source of error is the noise to the recorded signal due to the engine operation, the receiver and servos. One of the most significant

32

errors is the noise of the signal as discussed in [Ref. 7: pp. 45]. Therefore, RPM signal conditioning is an important factor for these flight tests.

To reduce the raw flight test data, the signal conditioning wave shaper was used. Before using the wave shaper to condition the signal, the output data was dependent upon the sensitivity level setting of the frequency counter and the volume level of the recorder. The unconditioned frequency had fluctuations of ±50 Hz which was 13.3 % off from the average take-off frequency of 360 Hz. The frequency counter counted the frequency of the rectangular pulse signals from the wave shaper with only ±8 Hz fluctuation of the take-off frequency(360 Hz). This is only 2.2 % in error. Also, this frequency output fluctuation could be reduced by averaging the data which corresponded to one frequency band. Thirteen to eighteen data points were used to get the average frequency. Averaging the output would be easier with a print out of the output frequency data. Alternatively, using a recorder, it is possible to average a larger amount of data. In this investigation the alternative method was used to get the average frequency data. Another error source could be a wind factor. The aircraft true airspeed was determined by averaging the velocity calculated for each direction flown for the entire range of throttle settings. Flight testing was performed in the morning to take advantage of the low winds. The greatest cross wind velocity measured during flight testing was a steady 3 - 4 kts with gusts up to 6 kts and 45 degree cross wind direction. In this case the error of the true airspeed due to cross wind turned out to be less than 0.5 %. Therefore the effect could be negligible.

B. FLIGHT TEST RESULTS WITH MODIFIED WING CONFIGURATION

The raw flight test data with the modified wing configuration are listed in Table 17 on page 54 in Appendix B. The data for the aircraft characteristics of the modified configuration is listed in Table 18 on page 55 and Table 19 on page 55 at Appendix B. The drag-polar for the original and modified wing configuration is shown in Figure 21.
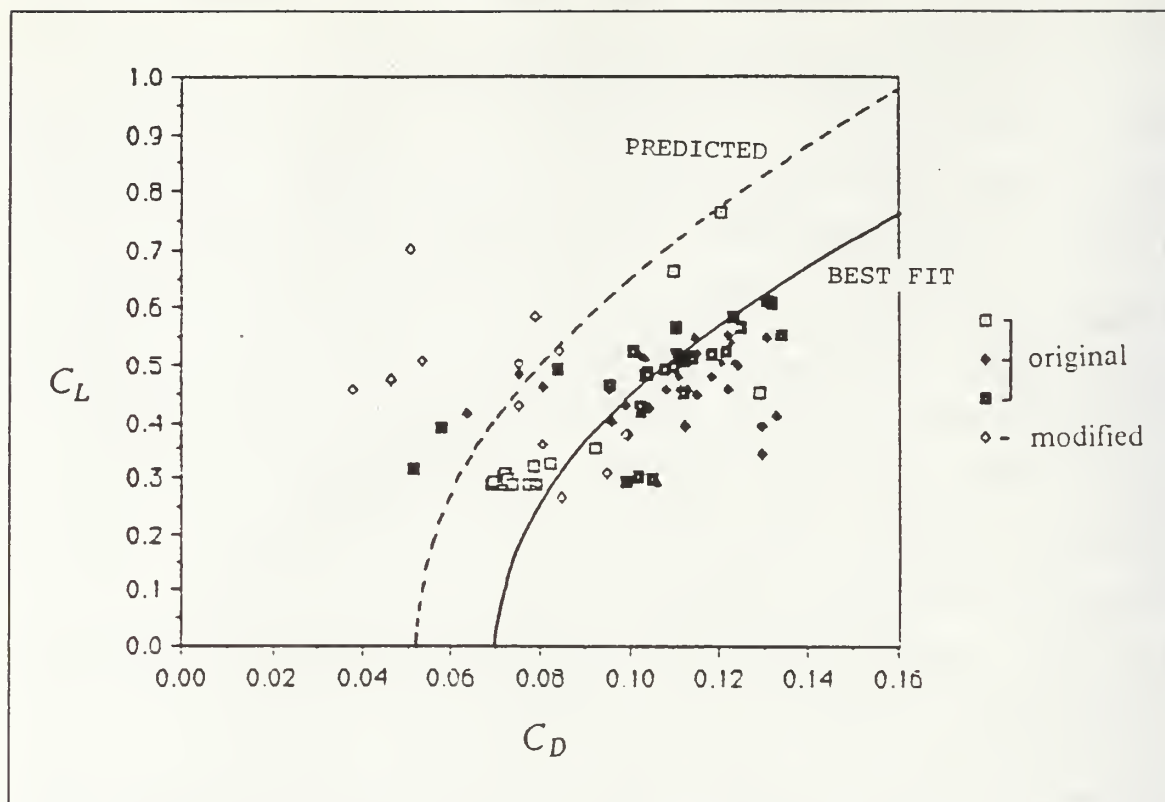
Figure 21. Drag-Polar For Original and Modified Wing Configuration

The number of data points from the modified wing configuration flight test were not enough to make a drag polar. For completion of the drag polar, more data are needed. This supplimentary flight test will be continued in the third-phase work. The results of the modified wing configuration are much closer to the predicted drag polar, though the scatter is large. Therefore, the half-scale Pioneer has a better characteristics with the modified wing configuration. But the data points show a large distribution. For more accurate analysis, the large distribution of the results could be reduced with more accurate measurements. The large scatter problem can be improved by using an airspeed indicator, as will be done in the third-phase flight tests of the half-scale Pioneer.

VI. CONCLUSIONS AND RECOMMENDATIONS

Flight tests were performed with the original configuration and with the wing modified to reduce wing skin-friction and the trailing edge separation drag. The following conclusions were reached:

(1) Flight test data indicate a higher drag than predicted by panel-method simulation. Trends indicate that the induced drag was predicted fairly well. Values for parasite drag were 20-25 % higher than predicted.

(2) Data from the flights with the modified wing indicate that an actual benefit can be realized from improving the wing surface and airfoil contour.

(3) The scatter of data is almost unacceptable. Errors due to the method of determining airspeed, and the RPM measurements, are most likely the causes of the large scatter.

The following recommendations for the next phase of the flight test are:

(1) Install an airspeed indicator for better and more accurate speed resolution.

(2) Acquire additional data for the improved-wing condition.

(3) Perform flight test with the boundary layer tripped to compare the original work with the smooth wing and the wing with a fully-turbulent boundary layer.

(4) Continue to install and check-out additional instrumentation for future stability-and-control flight test.

APPENDIX A.   FLIGHT TEST DATA FROM FIRST-PHASE

In this section the results from the first-phase are listed. In the first-phase the flight test was conducted with the original aircraft configuration by Tanner[Ref. 8]. Tanner developed a flight test procedure and established the data reduction from the torque stand and wind tunnel tests. The following data came from his thesis, which are used for the approach to aerodynamic analysis of the half-scale Pioneer in the second phase. Also another approach to the half-scale Pioneer was made in the first phase by Lyons who used the analytical method of Hoerner's drag estimation. Lyons studied the full-scale Pioneer, but he also examined the half-scale Pioneer. This section is based on the comparison between the first phase work and the second-phase work.

A.   FLIGHT TEST RESULTS FROM THE FIRST PHASE

1.   Torque stand and Wind Tunnel Test Results

Torque stand and the wind tunnel tests were performed to obtain propeller efficiency data and thrust coefficient data which was conducted by Tanner in the first-phase of the half-scale Pioneer flight test. The wind tunnel test results are listed in Table 5 on page 37.

Table 5.   PROPELLER EFFICIENCY DATA

n(RPM)	J	T_E	SBHP(hp)	η
4400	0.6177	0.120	0.083	15.11
4500	0.6568	0.219	0.096	23.84
4700	0.6289	0.417	0.124	35.14
4900	0.6032	0.764	0.152	52.58
5100	0.5795	0.862	0.179	50.32
5400	0.5473	1.368	0.231	61.37
5600	0.5278	1.605	0.255	65.77
5800	0.5096	1.952	0.308	66.22
6200	0.4767	2.545	0.403	65.82
6500	0.4547	3.139	0.479	68.48
6900	0.4284	3.931	0.590	69.62
7400	0.3994	4.870	0.714	71.27
7700	0.3839	5.513	0.800	72.01
8100	0.3649	6.403	0.910	73.52
8300	0.3561	6.748	0.971	72.62
8500	0.3477	7.293	1.055	72.58

The effective thrust coefficient was obtained with respect to the advance ratio as listed in Table 6 on page 38.

Table 6.   WIND TUNNEL DATA

n(RPM)	J	T_E	C_{T_E}
4400	0.612	0.120	0.0051
4500	0.657	0.219	0.0089
4700	0.629	0.417	0.0155
4900	0.603	0.764	0.0261
5100	0.580	0.862	0.0272
5400	0.547	1.358	0.0383
5600	0.528	1.605	0.0421
5800	0.510	1.952	0.0477
6200	0.477	2.545	0.0544
6500	0.455	3.139	0.0610
6900	0.428	3.931	0.0678
7400	0.399	4.870	0.0731
7700	0.384	5.513	0.0764
8100	0.365	6.403	0.0802
8300	0.356	6.748	0.0805
8500	0.348	7.293	0.0829

2.   Flight Test Data

The flight test results with the original wing surface of the half-scale Pioneer are listed in Table 7 on page 39, Table 8 on page 40, Table 9 on page 43, Figure 22, Figure 23, Figure 24 and Figure 25. These data have been used to compare with the second-phase work.

Table 7.   FLIGHT TEST DATA

Thr'(%)	V_T	n(RPM)	W_T	J	η	$SBHP_{STD}$	C_T	T
25	60.77	7150	26.50	0.44	70.7	0.728	0.1233	4.139
30	65.38	7500	26.55	0.45	70.2	0.870	0.1131	4.391
35	79.40	9525	26.60	0.43	70.9	1.054	0.1328	7.604
40	89.74	9830	26.65	0.47	69.3	1.140	0.0952	6.967
45	93.42	9950	26.70	0.48	68.8	1.240	0.0862	6.836
50	94.66	9960	26.75	0.49	67.8	1.350	0.0804	6.542
55	96.67	9975	26.80	0.50	67.0	1.398	0.0736	6.249
60	96.96	9995	26.40	0.50	67.0	1.445	0.0735	6.274
65	97.52	10050	26.45	0.50	67.0	1.469	0.0734	6.343
70	97.84	10110	26.50	0.50	67.0	1.495	0.0738	6.419
75	98.44	10220	26.55	0.50	67.0	1.524	0.0745	6.560
80	99.00	10220	26.60	0.50	67.0	1.545	0.0734	6.534
85	99.28	10150	26.65	0.50	67.0	1.544	0.0732	6.470
90	99.50	10325	26.70	0.50	67.0	1.555	0.0744	6.695
95	99.73	10520	26.75	0.49	67.8	1.578	0.0807	7.298
100	99.89	10480	26.80	0.49	67.8	1.590	0.0799	7.243

Table 8.   DRAG POLAR DATA(POWER AND THRUST METHOD)

THROT-TLE(%)	Power Method		Thrust Method	
	C_L	C_D	C_L	C_D
25	0.790	0.1430	0.790	0.1233
30	0.684	0.1362	0.684	0.1131
35	0.465	0.0931	0.465	0.1328
40	0.364	0.0682	0.364	0.0952
45	0.337	0.0653	0.337	0.0862
50	0.329	0.0673	0.329	0.0804
55	0.316	0.0646	0.316	0.0736
60	0.309	0.0662	0.309	0.0735
65	0.306	0.0661	0.306	0.0734
70	0.305	0.0667	0.305	0.0738
75	0.302	0.0668	0.302	0.0645
80	0.299	0.0665	0.299	0.0734
85	0.298	0.0659	0.298	0.0722
90	0.297	0.0659	0.297	0.0744
95	0.296	0.0672	0.296	0.0807
100	0.296	0.0674	0.296	0.0799
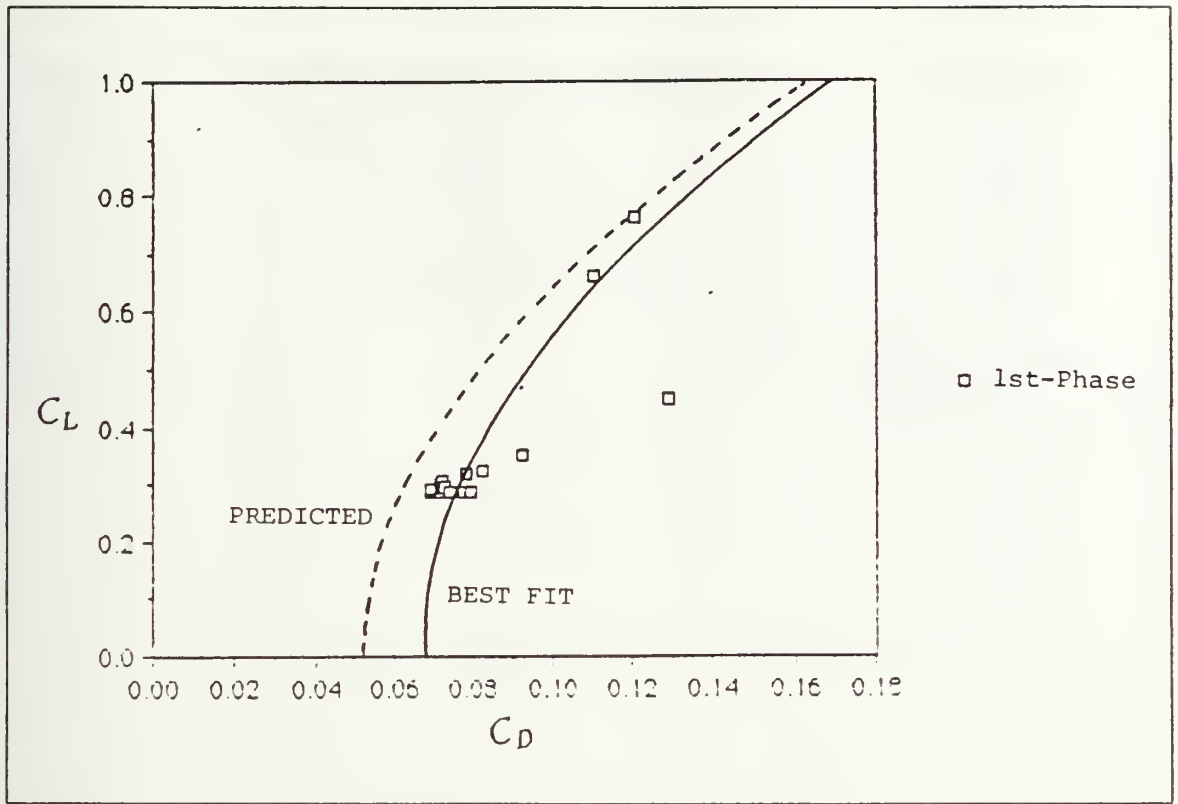
Figure 22.   Half-Scale Pioneer Drag Polar Curve(Thrust Method)
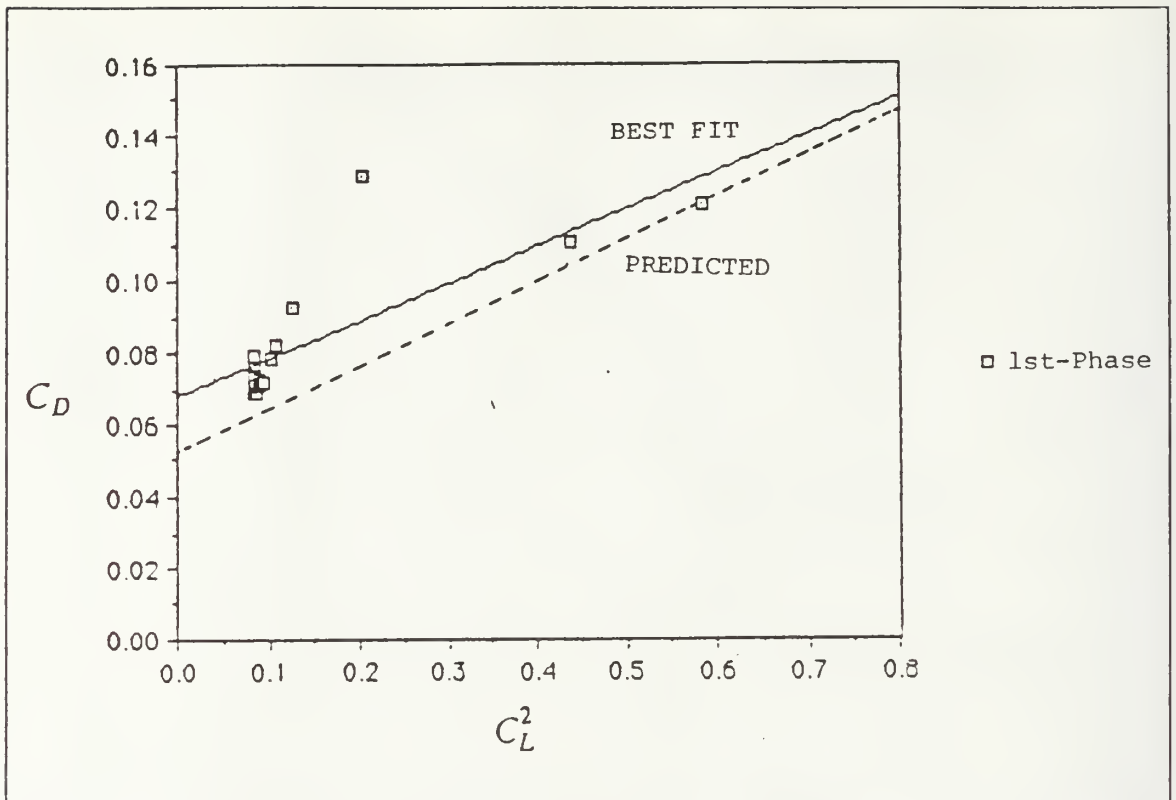
Figure 23. Drag Polar Linear Regression Plot(Thrust Method)

Table 9.   POWER REQUIRED DATA(POWER AND THRUST METHOD)

THROT-TLE(%)	Power Method		Thrust Method	
	P_{ra}	V_{ia}	P_{ra}	V_{ia}
25	0.540	61.75	0.790	61.75
30	0.639	66.37	0.684	66.37
35	0.780	80.50	0.465	80.50
40	0.822	90.92	0.364	90.92
45	0.885	94.56	0.337	94.56
50	0.947	95.72	0.329	95.72
55	0.966	97.68	0.316	97.68
60	1.021	98.70	0.309	98.70
65	1.036	99.20	0.306	99.20
70	1.051	99.41	0.305	99.41
75	1.068	99.92	0.302	99.92
80	1.080	100.41	0.299	100.41
85	1.076	100.60	0.298	100.60
90	1.081	100.72	0.297	100.72
95	1.107	100.87	0.296	100.87
100	1.112	100.94	0.296	100.94
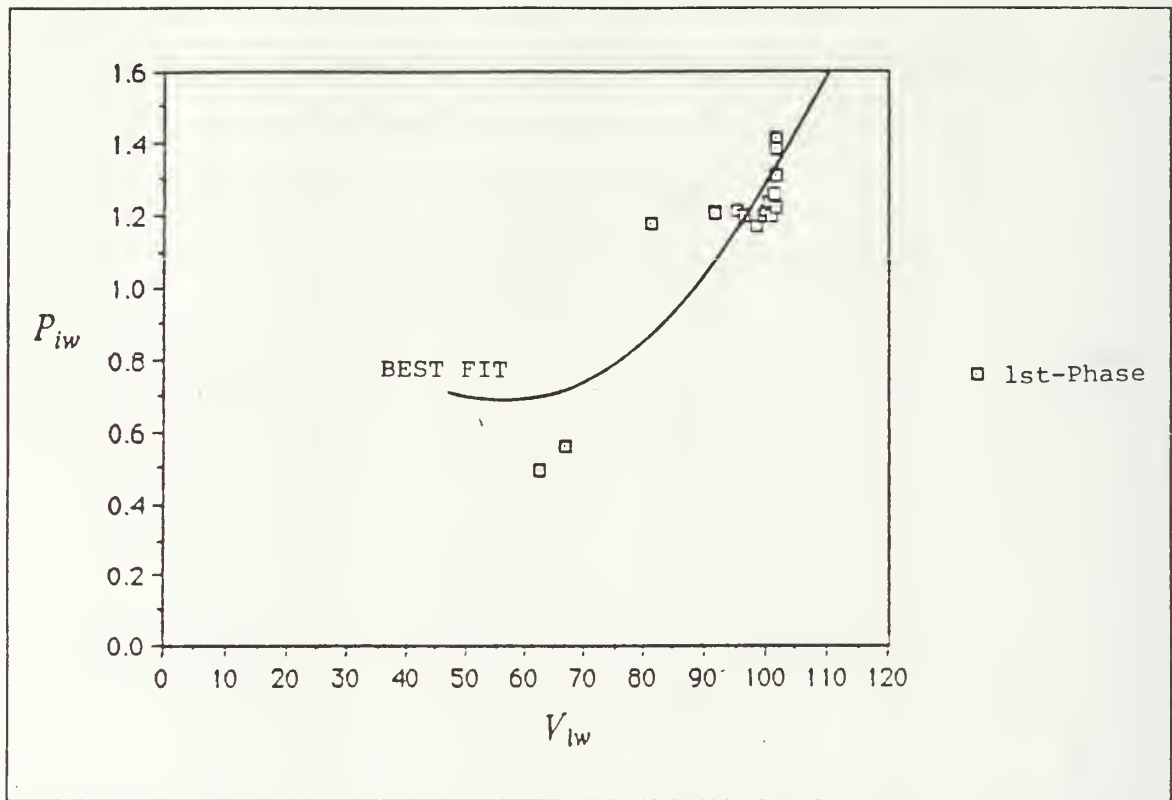
Figure 24.   Half-Scale Pioneer Power Required Curve(Thrust Method)
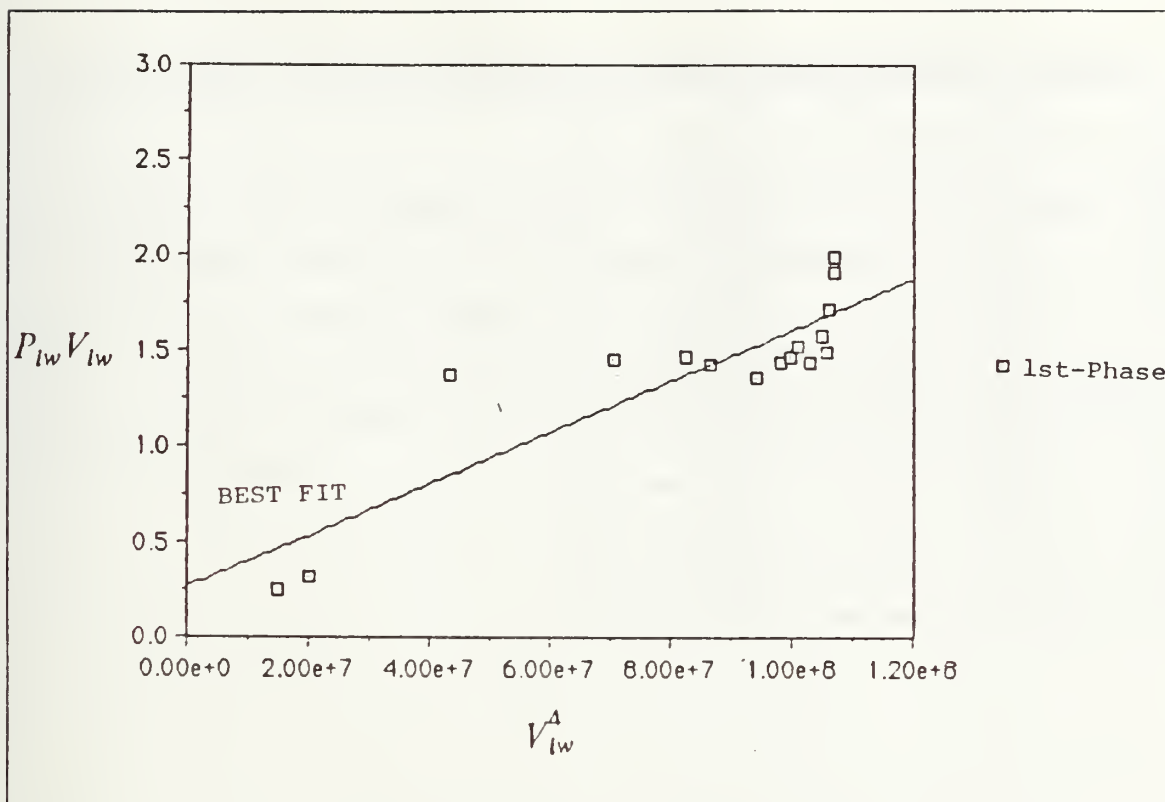
Figure 25.   Power Required Linear Regression Plot(Thrust Method)

B. DRAG ESTIMATION OF HALF-SCALE PIONEER WITH HOERNER'S DRAG ANALYSIS

Lyons developed a method of the analytical drag estimation of the half-scale Pioneer. The results of the predicted drag are listed in Table 10 on page 46 and the result can be reduced to a drag-polar equation as $C_D = 0.0521 + 0.1142C_L^2$. The predicted drag-polar is shown by the dotted line in Figure 17 and Figure 18.

Table 10.   PREDICTED DRAG ANALYSIS DATA

C_L	C_D
0.00	0.0521
0.10	0.0532
0.20	0.0567
0.30	0.0624
0.40	0.0704
0.50	0.0806
0.60	0.0932
0.70	0.1081
0.80	0.1252
0.90	0.1446
1.00	0.1663

APPENDIX B.   FLIGHT TEST RESULTS FROM SECOND-PHASE

This section includes the results of the second-phase flight test. The data tables are raw flight test data, reduced data and the aircraft characteristics data.

In the raw data table, T_a is a measured flight time for the 1500-foot distance in one direction, T_b is the other measured time for opposite direction flight, F_a is the corresponding frequency of the engine revolutions for the flight time T_a and the F_b is the opposite direction frequency.

Table 11.   SUPPLIMENTARY FLIGHT TEST RAW DATA (19 AUG.)

RUN NO.	T_a	T_b	F_a	F_b	W_T
1	16.13	18.05	355.0	349.5	27.55
2	17.17	19.02	346.3	344.2	27.5
3	16.30	18.20	316.3	313.0	27.45
4	19.25	18.00	302.3	306.3	27.4
5	20.06	19.35	289.8	294.7	27.8
6	19.20	19.02	292.0	292.1	27.75
7	19.01	19.18	291.6	292.2	27.7
8	15.76	17.97	327.7	326.5	27.65
9	15.82	17.58	343.3	344.0	27.6
10	17.21	16.13	360.4	355.2	27.55
11	14.66	16.48	381.6	383.6	27.5
12	14.13	14.47	397.0	390.9	27.45
13	18.03	17.85	327.6	325.0	27.8
14	18.22	17.66	320.9	318.1	27.75
15	19.33	19.03	301.8	299.2	27.7
16	17.78	18.21	314.2	315.5	27.65
17	18.16	17.41	324.3	324.3	27.6
18	16.72	16.02	337.0	341.1	27.55
19	17.35	17.34	323.7	323.4	27.5
20	17.93	17.00	317.1	317.6	27.45
21	19.32	18.87	294.8	291.5	27.4
22	19.13	16.47	317.7	318.7	27.6
23	19.34	17.57	312.3	306.9	27.55
24	19.87	18.06	312.5	309.2	27.5
25	20.34	17.62	310.4	313.3	27.45
26	19.13	17.89	312.9	314.9	27.4
27	20.77	18.44	298.9	301.3	27.6
28	21.75	18.63	295.9	294.4	27.55
29	20.30	17.76	307.5	308.6	27.5
30	20.35	19.24	303.1	300.6	27.45
31	20.72	17.91	301.1	297.5	27.4
					$P = 29.82 inHG$, $T = 65°F$

Table 12.   SUPPLIMENTARY FLIGHT TEST RAW DATA (26 AUG.)

RUN NO.	T_a	T_b	F_a	F_b	W_T
1	18.86	21.34	305.0	283.4	27.55
2	20.38	20.49	286.9	287.9	27.5
3	18.75	19.66	298.6	299.3	27.45
4	18.76	19.57	298.3	298.0	27.4
5	17.36	18.69	316.8	318.8	27.35
6	16.94	18.12	318.6	319.5	27.3
7	18.34	19.12	299.7	298.9	27.25
8	19.85	20.53	282.4	282.1	27.2
9	20.63	21.25	286.3	285.6	27.15
10	21.37	20.77	282.9	283.9	27.1
11	14.25	14.59	388.7	391.0	27.8
12	13.73	15.06	387.7	383.0	27.75
13	13.94	15.38	381.0	381.5	27.7
14	14.81	14.99	372.2	370.0	27.65
15	15.81	17.56	346.5	342.4	27.6
16	16.63	17.81	324.7	324.8	27.55
17	17.91	19.65	282.5	284.3	27.5
18	18.76	19.94	286.2	289.0	27.45
19	18.47	20.01	292.0	298.6	27.4
20	18.72	21.15	300.5	305.3	27.35
21	17.19	21.03	304.1	303.0	27.55
22	17.57	20.00	303.1	301.9	27.5
23	17.53	20.25	302.5	302.9	27.45
24	17.44	19.94	301.8	300.6	27.4
25	16.68	20.00	301.0	302.1	27.35
26	17.23	21.26	300.3	301.0	27.3
27	17.50	21.12	300.2	300.5	27.25
28	18.19	20.74	300.0	299.5	27.2
29	17.22	20.76	300.0	301.2	27.15
					$P = 29.82 in HG$. $T = 65°F$

Table 13.   SUPPLIMENTARY FLIGHT TEST DATA (19 AUG.)

NO.	V_T	n	J	C_{T_E}	T_E
1	88.05	10568	0.428	0.0668	9.012
2	83.11	9116	0.469	0.0575	5.769
3	87.22	8709	0.515	0.0461	4.220
4	80.63	8358	0.496	0.0508	4.289
5	76.15	8768	0.447	0.0627	5.822
6	78.49	8762	0.461	0.0594	5.510
7	83.19	8757	0.489	0.0527	4.881
8	89.33	9813	0.468	0.0577	6.707
9	90.07	10310	0.449	0.0621	7.972
10	90.08	10734	0.432	0.0661	9.204
11	96.67	11478	0.433	0.0658	10.454
12	104.91	11819	0.506	0.0483	8.158
13	83.61	9789	0.439	0.0644	7.454
14	83.63	9585	0.449	0.0622	6.906
15	78.21	9015	0.446	0.0628	6.167
16	83.37	9446	0.454	0.0610	6.576
17	84.38	9729	0.446	0.0628	7.186
18	91.67	10172	0.463	0.0588	7.344
19	86.48	9706	0.458	0.0600	6.831
20	85.95	9521	0.464	0.0586	6.414
21	78.57	8795	0.459	0.0597	5.580
22	83.55	9546	0.450	0.0619	6.814
23	81.47	9288	0.451	0.0617	6.428
24	79.27	9326	0.437	0.0649	6.814
25	79.44	9356	0.437	0.0650	6.870
26	81.13	9417	0.443	0.0635	6.806
27	76.78	9003	0.439	0.0645	6.320
28	75.55	8855	0.439	0.0645	6.108
29	79.18	9242	0.441	0.0641	6.612
30	75.84	9056	0.431	0.0663	6.570
31	78.07	8979	0.447	0.0626	6.095

Table 14. SUPPLIMENTARY FLIGHT TEST DATA (26 AUG.)

NO.	V_T	n	J	C_{T_F}	T_F
1	74.91	8826	0.437	0.0650	6.104
2	73.40	8622	0.438	0.0647	5.798
3	78.15	8969	0.448	0.0624	6.046
4	78.30	8945	0.450	0.0619	5.967
5	83.33	9534	0.450	0.0620	6.797
6	85.66	9572	0.460	0.0595	6.573
7	80.12	8979	0.459	0.0599	5.816
8	74.32	8468	0.451	0.0616	5.324
9	71.65	8579	0.430	0.0666	5.905
10	71.21	8502	0.431	0.0663	5.777
11	104.04	11696	0.457	0.0602	9.922
12	104.43	11561	0.465	0.0585	9.425
13	102.57	11438	0.461	0.0593	9.351
14	100.67	11133	0.465	0.0584	8.723
15	90.15	10334	0.449	0.0622	8.010
16	87.21	9743	0.460	0.0595	6.8.7
17	80.04	8502	0.484	0.0538	4.685
18	77.59	8628	0.462	0.0590	5.294
19	77.72	8859	0.451	0.0617	5.833
20	75.53	9087	0.427	0.0670	6.672
21	79.29	9107	0.448	0.0624	6.241
22	80.19	9075	0.454	0.0609	6.045
23	79.82	9081	0.452	0.0615	6.108
24	80.62	9036	0.459	0.0599	5.891
25	82.46	9047	0.469	0.0575	5.672
26	78.81	9020	0.449	0.0621	6.087
27	78.37	9012	0.447	0.0626	6.125
28	68.27	8993	0.390	0.0749	7.296
29	80.57	9018	0.459	0.0597	5.853

Table 15.   DRAG POLAR AND POWER REQUIRED DATA (19 AUG.)

NO.	C_L	C_D	P_{iw}	V_{iw}
1	0.406	0.1329	1.450	88.19
2	0.455	0.0955	0.878	83.32
3	0.413	0.0634	0.676	87.52
4	0.482	0.0754	0.637	80.98
5	0.548	0.1148	0.799	75.93
6	0.515	0.1022	0.782	78.34
7	0.458	0.0806	0.736	83.10
8	0.396	0.0961	1.089	89.31
9	0.339	0.1123	1.308	90.13
10	0.388	0.1297	1.515	90.22
11	0.336	0.1281	1.854	96.91
12	0.285	0.0847	1.572	105.27
13	0.455	0.1219	1.123	83.37
14	0.454	0.1129	1.044	83.46
15	0.518	0.1153	0.874	78.12
16	0.461	0.1082	0.996	83.35
17	0.443	0.1154	1.105	84.44
18	0.375	0.0999	1.230	91.82
19	0.420	0.1044	1.082	86.70
20	0.425	0.0993	1.013	86.24
21	0.507	0.1034	0.808	78.91
22	0.452	0.1116	1.037	83.61
23	0.475	0.1107	0.957	81.60
24	0.500	0.1240	0.990	79.47
25	0.597	0.1245	1.003	79.71
26	0.476	0.1182	1.017	81.48
27	0.535	0.1225	0.884	76.84
28	0.552	0.1223	0.843	75.67
29	0.502	0.1206	0.959	79.38
30	0.546	0.1306	0.915	76.10
31	0.514	0.1143	0.878	78.41

52

Table 16.   DRAG POLAR AND POWER REQUIRED DATA (26 AUG.)

NO.	C_L	C_D	P_{m}	V_{m}
1	0.563	0.1246	0.832	74.94
2	0.585	0.1233	0.777	73.50
3	0.515	0.1134	0.865	78.32
4	0.512	0.1115	0.858	78.55
5	0.451	0.1122	1.042	83.67
6	0.426	0.1026	1.039	86.09
7	0.486	0.1038	0.862	80.59
8	0.564	0.1105	0.734	74.82
9	0.606	0.1318	0.787	72.21
10	0.612	0.1306	0.768	71.83
11	0.294	0.1050	1.854	103.61
12	0.292	0.0990	1.772	104.09
13	0.302	0.1019	1.732	102.33
14	0.313	0.0986	1.590	100.54
15	0.389	0.1129	1.311	90.11
16	0.415	0.1026	1.081	87.25
17	0.492	0.0838	0.684	80.15
18	0.522	0.1007	0.752	77.77
19	0.520	0.1106	0.832	77.96
20	0.549	0.1340	0.927	75.83
21	0.502	0.1137	0.901	79.33
22	0.490	0.1077	0.885	80.29
23	0.494	0.1098	0.892	80.00
24	0.483	0.1039	0.872	80.87
25	0.461	0.0956	0.861	82.80
26	0.504	0.1123	0.885	79.20
27	0.508	0.1143	0.888	78.83
28	0.669	0.1794	0.924	68.74
29	0.479	0.1034	0.876	81.20

Table 17. FLIGHT TEST RAW DATA WITH CHANGED WING CONFIG-URATION (16 SEP.)

RUN NO.	T_a	T_b	F_a	F_b	W_T
1	13.19	15.03	388.1	385.6	28.55
2	14.12	16.39	369.3	369.2	28.5
3	13.62	16.06	367.6	359.2	28.45
4	15.59	17.84	342.1	338.5	28.8
5	15.41	17.00	329.7	334.8	28.75
6	17.40	18.13	297.1	298.0	28.7
7	17.44	19.28	254.9	249.1	28.65
8	18.06	19.28	255.5	256.7	28.6
9	21.38	24.38	214.7	211.9	28.55
10	19.03	19.63	257.6	250.0	28.5
11	19.17	22.75	251.2	262.8	28.45
12	19.35	19.31	271.6	275.3	28.4
13	19.06	20.56	267.4	281.8	28.35
				row1. row2. row3	$P = 29.89inHg$, $T = 63.2°F$
				rest of rows	$P = 29.72inHg$, $T = 69°F$

54

Table 18. FLIGHT TEST DATA WITH CHANGED WING CONFIGURATION (16 SEP.)

NO.	V_T	n	J	C_{T_F}	T_E
1	106.80	11605	0.473	0.0565	9.219
2	98.88	11078	0.459	0.0598	8.897
3	101.8	10902	0.480	0.0548	7.892
4	90.15	10209	0.454	0.0610	7.575
5	92.79	9968	0.479	0.0551	6.525
6	84.47	8927	0.487	0.0532	5.050
7	81.91	7560	0.557	0.0352	2.396
8	80.43	7683	0.538	0.0401	2.819
9	65.84	6399	0.529	0.0425	2.072
10	77.62	7614	0.524	0.0437	3.020
11	72.09	7710	0.481	0.0546	3.868
12	77.60	8204	0.486	0.0532	4.268
13	75.83	8238	0.473	0.0564	4.562

Table 19. DRAG POLAR AND POWER REQUIRED DATA (16 SEP.)

NO.	C_L	C_D	P_m	V_m
1	0.262	0.0846	1.713	105.22
2	0.305	0.0952	1.535	97.54
3	0.287	0.0797	1.405	100.48
4	0.377	0.0991	1.144	82.73
5	0.355	0.0806	1.017	90.37
6	0.428	0.0752	0.718	82.35
7	0.454	0.0380	0.331	79.91
8	0.471	0.0463	0.384	78.54
9	0.700	0.0508	0.232	64.35
10	0.503	0.0533	0.399	75.93
11	0.582	0.0791	0.476	70.58
12	0.501	0.0754	0.576	76.05
13	0.524	0.0844	0.594	74.37

LIST OF REFERENCES

1. Von Karman Institute, *Lecture Note Series 101*, 1964.

2. James C. Tanner, *Development of a Flight Test Methodology for A U.S.Navy Half-Scale Unmanned Air Vehicle*, Naval Postgraduate School, Mar., 1989.

3. Daniel F. Lyons, *Aerodynamic Analysis of A U.S. Navy and Marine Corps Unmanned Air Vehicle*, Naval Postgraduate School, Jun., 1989.

4. Sean C. Roberts, *Light Aircraft Performance for test Pilots and Flight Test Engineers*, Flight Research, Inc., 1982.

5. John D. Anderson, Jr., *Introduction to Flight*, McGraw-Hill Book Company, 1985.

6. AGARD, *Flight Test Manual Vol. 1 Performance*.

7. Nicolaos D. Bamichas, *Flight Test Method Development For A Quarter-Scale Aircraft With Minimum Instrumentation*, Naval Postgraduate School Master's Thesis, Mar., 1989.

8. Wilbur C. Nelson, *Airplane-Propeller Principles*, John Wiley and Sons, Inc., 1944.

INITIAL DISTRIBUTION LIST

10. 3rd Department of Air Force College   1
    Chongwon-Gun, Chungbook-Do,
    Republic of Korea

11. Library of Air Force Academy   2
    Chongwon-Gun, Chungbook-Do,
    Republic of Korea

12. Kwon, Himan   2
    SMC 1375, NPS
    Monterey, CA 93943-5000

13. Higman, Jerry   1
    SMC 1359, NPS
    Monterey, CA 93943-5000

14. Kee, Yeho   5
    67 Hyangsan-ri, Gochon-myon, Kyeunggi-do,
    Republic of Korea